ATMOSPHERIC BRIDGE, OCEANIC TUNNEL, AND GLOBAL CLIMATIC TELECONNECTIONS

Zhengyu Liu[1] and Mike Alexander[2]

Received 25 April 2005; revised 25 June 2006; accepted 4 December 2006; published 23 June 2007.

[1] We review teleconnections within the atmosphere and ocean, their dynamics and their role in coupled climate variability. We concentrate on teleconnections in the latitudinal direction, notably tropical-extratropical and interhemispheric interactions, and discuss the timescales of several teleconnection processes. The tropical impact on extratropical climate is accomplished mainly through the atmosphere. In particular, tropical Pacific sea surface temperature anomalies impact extratropical climate variability through stationary atmospheric waves and their interactions with midlatitude storm tracks. Changes in the extratropics can also impact the tropical climate through upper ocean subtropical cells at decadal and longer timescales. On the global scale the tropics and subtropics interact through the atmospheric Hadley circulation and the oceanic subtropical cell. The thermohaline circulation can provide an effective oceanic teleconnection for interhemispheric climate interactions.

Citation: Liu, Z., and M. Alexander (2007), Atmospheric bridge, oceanic tunnel, and global climatic teleconnections, *Rev. Geophys.*, *45*, RG2005, doi:10.1029/2005RG000172.

1. INTRODUCTION

[2] Teleconnection generally refers to the linkage of seemingly unrelated climate anomalies over great distances. Although the notion of teleconnection was recognized many years before [e.g., *Hildebrandsson*, 1897; *Walker*, 1924], the first known use of "teleconnections" was by *Ångström* [1935] in reference to the north-south dipole atmospheric anomaly pattern now referred to as the North Atlantic Oscillation (NAO). *Wallace and Gutzler* [1981] defined teleconnections as significant simultaneous correlations between temporal fluctuations in meteorological parameters at widely separated points on Earth. Many of the teleconnection patterns that they identified were regional in nature and shaped by wave processes. Here we generalize the concept of teleconnection to include zonal mean anomalies and connections via other components of the climate system, especially the ocean. This generalization is useful because the essence of teleconnection is that it allows a climatic event to affect the Earth system elsewhere. The resulting interactions between different regions contribute greatly to the complexity of the climate system. Therefore a broad definition of teleconnection allows us to think about the climate variability of various spatial and temporal scales in a more unified framework.

[3] Teleconnections are caused by energy transport and wave propagation in the atmosphere and ocean. Teleconnections enable the atmosphere to act like a "bridge" between different parts of the ocean and enable the ocean to act like a "tunnel" linking different atmospheric regions. Of particular interest here are interactions in the meridional direction, notably between the tropics and extratropics, between the middle and high latitudes, and between the two hemispheres. Although necessary for balancing the equator-pole difference in solar radiation, latitudinal teleconnections are nontrivial, because the atmosphere and ocean tend to flow zonally as constrained by the conservation of angular momentum (or potential vorticity). In this paper, we summarize the progress that has been made over the last 25 years in our understanding of teleconnections and their role in coupled climate variability.

[4] Historically, meridional teleconnections were implicitly considered in the long-term energy balance of the global climate system. Solar insolation decreases from 450 W m^{-2} at the equator to 200 W m^{-2} at the pole; to maintain the present-day temperature structure under this forcing requires a poleward heat transport of about 5 PW (1 PW = 10^{15} W) [*Vonder Haar and Oort*, 1973; *Hastenrath*, 1982; *Peixoto and Oort*, 1992; *Keith*, 1995; *Trenberth and Solomon*, 1994; *Trenberth and Caron*, 2001]. With a large uncertainty [*Wunsch*, 2005], current estimates suggest that the atmosphere and ocean transport approximately equal amounts of heat within 30° of the equator. In the atmosphere the excessive heating in the tropics drives an overturning Hadley cell (Figure 1), which transports energy to the

[1]Center for Climatic Research, University of Wisconsin-Madison, Madison, Wisconsin, USA.
[2]Physical Science Division, Earth System Research Laboratory, NOAA, Boulder, Colorado, USA.

8755-1209/06/2005RG000172
Paper number 2005RG000172

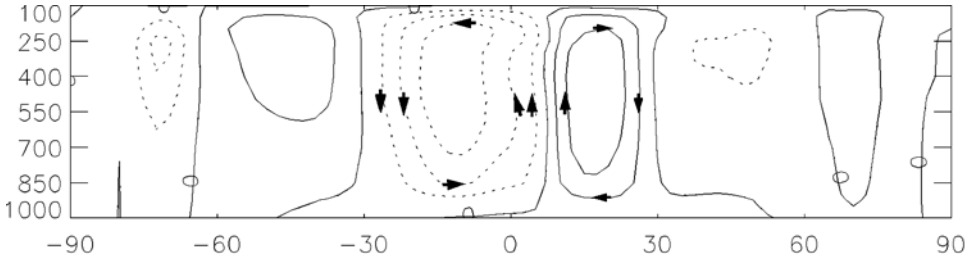

Figure 1. Annual mean Hadley cells in the Northern and Southern hemispheres (arrows) as represented by the stream function of the zonal average of the meridional wind and vertical motion obtained from the National Centers for Environmental Prediction (NCEP) reanalysis (a combination of model and data output [*Kalnay et al.*, 1996; *Kistler et al.*, 2001]) for the years 1948–2001. Contour interval is 2 × 1010 kg s^{-1}. From *Quan et al.* [2004, Figure 3.3], with kind permission from Springer Science and Business Media.

subtropics; the energy is then relayed poleward by synoptic storms that are generated by the unstable midlatitude westerly jet. In the ocean, high-latitude cooling induces an overturning thermohaline circulation (THC) (Figure 2), which transports heat poleward. The atmospheric wind stress also drives extratropical ocean gyres, which enhances the poleward heat transport. Without these heat transports the atmosphere would have an equator-pole surface air temperature difference of 100°C, which is more than twice the present value of 40°C [*Lindzen*, 1990].

[5] Atmospheric teleconnection patterns can be generated by both internal atmospheric processes and forcing from surface conditions, especially sea surface temperature (SST) anomalies associated with El Niño–Southern Oscillation (ENSO). During El Niño events the anomalous warming of the equatorial Pacific Ocean enhances tropical precipitation and generates atmospheric waves that emanate into the extratropics (Figure 3) [*Trenberth et al.*, 1998, and references therein]. These planetary waves form in preferred locations, resulting in quasi-stationary anomalies, such as

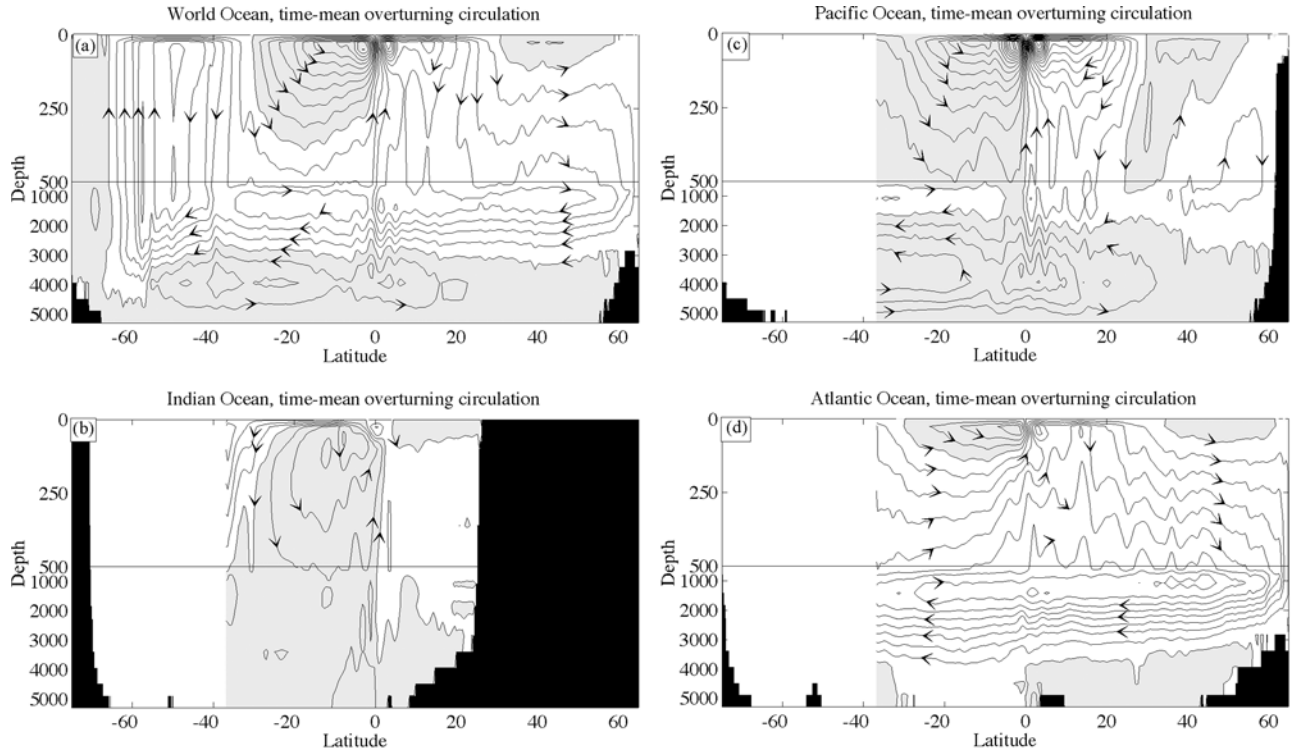

Figure 2. Time mean overturning circulation simulated in a 0.25° resolution global ocean general circulation model (Semtner and Tokmakian) for the (a) world, (b) Pacific, (c) Atlantic, and (d) Indian oceans. Negative values of the stream function are shaded and indicate counterclockwise overturning. Contour interval for the world ocean is 5 Sv, and the interval for the individual basins is 2.5 Sv. The model underestimates somewhat the Antarctic Bottom Water (AABW) in the Atlantic and may also underestimate the deep inflow into the Indian Ocean (J. Marotzke, personal communication, 2005). Adapted from *Jayne and Marotzke* [2001].

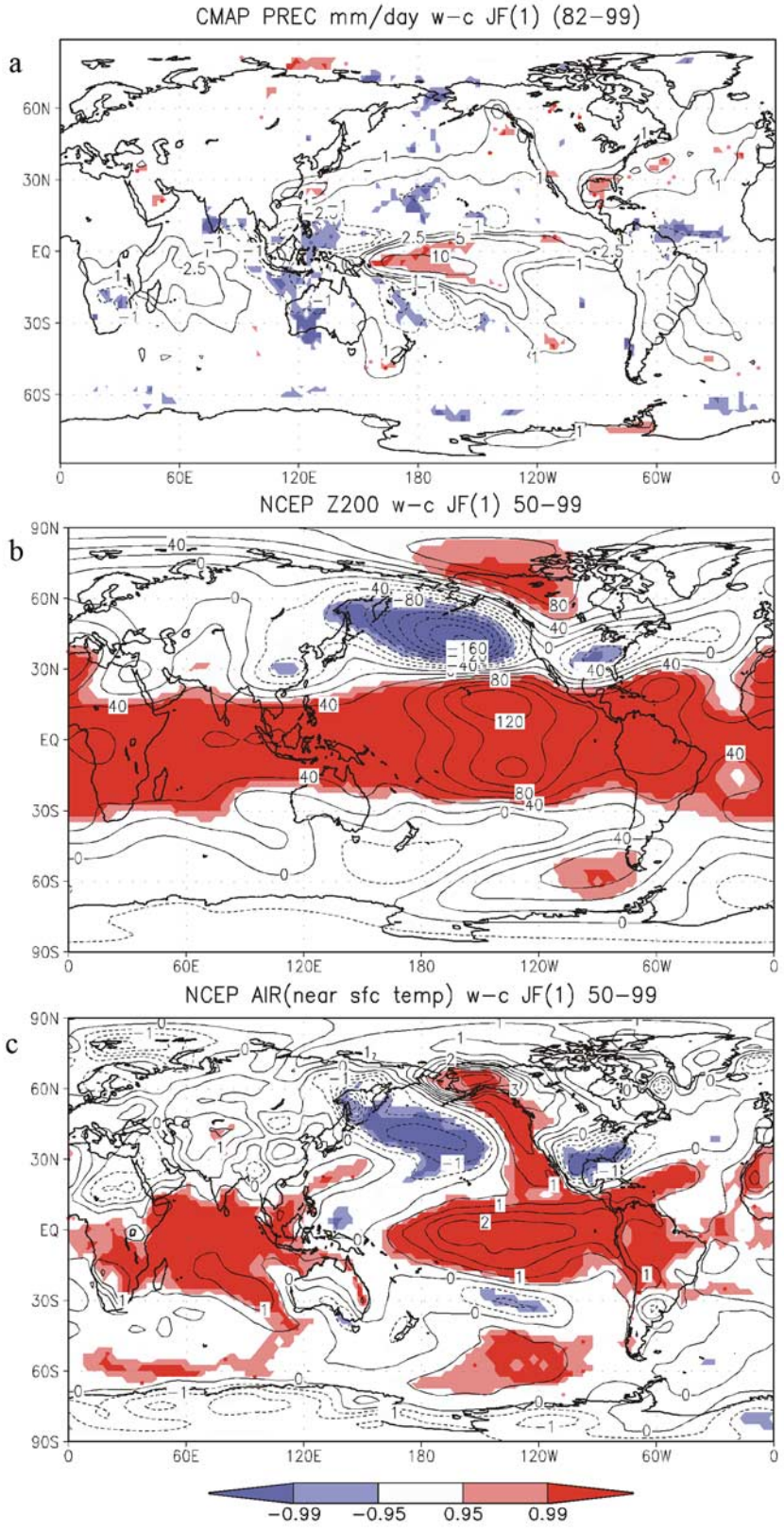
CMAP PREC mm/day w−c JF(1) (82−99)
a
NCEP Z200 w−c JF(1) 50−99
b
NCEP AIR(near sfc temp) w−c JF(1) 50−99
c
90N
60N
30N
EQ
30S
60S
90S
0
60E
120E
180
120W
60W
−0.99
−0.95
0.95
0.99

Figure 3

the Pacific–North America (PNA) pattern. Thus, in response to ENSO, the Aleutian Low strengthens over the North Pacific, high pressure and warm temperatures develop over western Canada, and precipitation is enhanced along the west coast and the southern tier of the United States during boreal winter (Figure 3). The ENSO-driven extratropical circulation anomalies, however, project on several different teleconnection patterns that vary with the seasons. ENSO-induced changes in air temperature, cloud cover, and wind can also impact the ocean far from the equatorial Pacific via fluxes of heat and momentum across the air-sea interface.

[6] In addition to tropically driven circulation anomalies, teleconnections can also extend from the middle and high latitudes to the tropics on interannual to decadal timescales. Several hypotheses for Pacific decadal variability (PDV) involve the extratropical impact on tropical climate either through the low-latitude portion of midlatitude atmospheric anomalies [e.g., *Barnett et al.*, 1999; *Vimont et al.*, 2001] or via the shallow subtropical cell (STC) in the ocean [*Gu and Philander*, 1997; *Kleeman et al.*, 1999]. The STC consists of a poleward warm surface Ekman flow, an equatorward cold compensating flow within the thermocline, and upwelling along the equator (top panels in Figures 2a–2c) [*McCreary and Lu*, 1994; *Liu et al.*, 1994]. The STC may serve as an ocean tunnel, especially on decadal timescales, through variations in the poleward heat transport in the tropics [*Marotzke and Klinger*, 2000; *Held*, 2001] and equatorward propagation of temperature anomalies in the thermocline (Figure 4).

[7] Past global climate changes suggest the occurrence of interhemispheric climate teleconnections [*Markgraf*, 2001]. One notable example is the hemispheric synchronicity of glacial cycles and millennia variability, which may be linked to THC changes in the North Atlantic [*Broecker*, 1998; *Shackleton*, 2000; *Marotzke*, 2000; *Stocker*, 2000; *Alley et al.*, 2002; *Lynch-Steiglitz*, 2004]. The ventilation of surface water into the deep North Atlantic appears to be over 1 km shallower at the Last Glacial Maximum (LGM) (which occurred ~21,000 years ago) than today, while the deep water from the Southern Ocean appears to penetrate much farther into the North Atlantic during the LGM as indicated by the distribution of benthic $\delta^{13}C$ [*Duplessy et al.*, 1988]. These past climate changes may have important implications for ocean heat transport, the carbon cycle, and global climate in the future, since most climate model simulations have suggested a significant reduction in the THC with an increase in the atmospheric CO_2 concentration [*Cubasch et al.*, 2001].

[8] The meridional extent and timescale of the teleconnection processes discussed above are summarized schematically in Figure 5. Teleconnections have a wide spectrum of timescales and therefore could impact climate variability in several different ways. Almost all atmospheric teleconnection processes are fast; that is, they reach equilibrium within a season, so they will be fully effective for climate variability on interannual and longer timescales. Oceanic processes, however, vary on interannual to decadal timescales for the upper ocean circulation and on decadal to millennial timescales for the thermohaline circulation and thus are only fully active for very low frequency climate variability.

[9] This paper will focus on the role of teleconnections in climate variability. We review the dynamics of atmospheric and oceanic teleconnections in sections 2 and 3, respectively. The roles of various teleconnection processes in coupled ocean-atmosphere-ice variability are discussed in section 4. Conclusions and additional discussions are given in section 5.

2. ATMOSPHERIC TELECONNECTIONS

[10] Changes in the Hadley cell, taken here to be the mean circulation averaged around a latitude band, can create zonally uniform atmospheric anomalies. Internal atmospheric processes, such as the interactions between the jet stream and midlatitude storm tracks, can result in both zonal and regional atmospheric anomalies. The atmospheric response to ENSO, and other boundary forcings, includes Rossby waves and localized eddy–mean flow interaction, which can both result in regional teleconnection patterns. In this section we explore the influence of the Hadley cell, stationary waves, and eddy–mean flow interactions on zonal and regional teleconnection patterns.

2.1. Zonally Symmetric Teleconnections

2.1.1. Hadley Cell

[11] The Hadley cell is a thermally direct circulation where heat from the Sun is converted to motion that transports energy from warm to cold regions. It extends from

Figure 3. El Niño (warm)–La Niña (cold) composite average of (a) precipitation (shaded interval is 0.25 mm d^{-1}, contours at ±1, 2.5, 5.0, and 10.0 mm d^{-1}), (b) 200 mb height (contour interval 20 m), and (c) near-surface air temperature during January and February (JF), where 0 indicates the year ENSO peaks and 1 indicates the following year. Shading indicates areas where the warm and cold composites are significantly different from each other at the 95% and 99% level as indicated by Monte Carlo resampling of the composite members. During El Niño events the precipitation is enhanced above and to the west of the anomalously warm water in the equatorial Pacific. The associated heating warms the tropical atmosphere and drives stationary patterns and storm track anomalies. The latter is indicated by the precipitation changes over the North Pacific and North Atlantic oceans. These ENSO-induced atmospheric changes force SST anomalies to form over the global oceans. The precipitation values are from the Climate Prediction Center Merged Analysis of Precipitation (CMAP) data set [*Xie and Arkin*, 1997] for ENSO events that occurred between 1979 and 2000, and the heights and temperature are from NCEP reanalysis for events between 1950 and 2000.

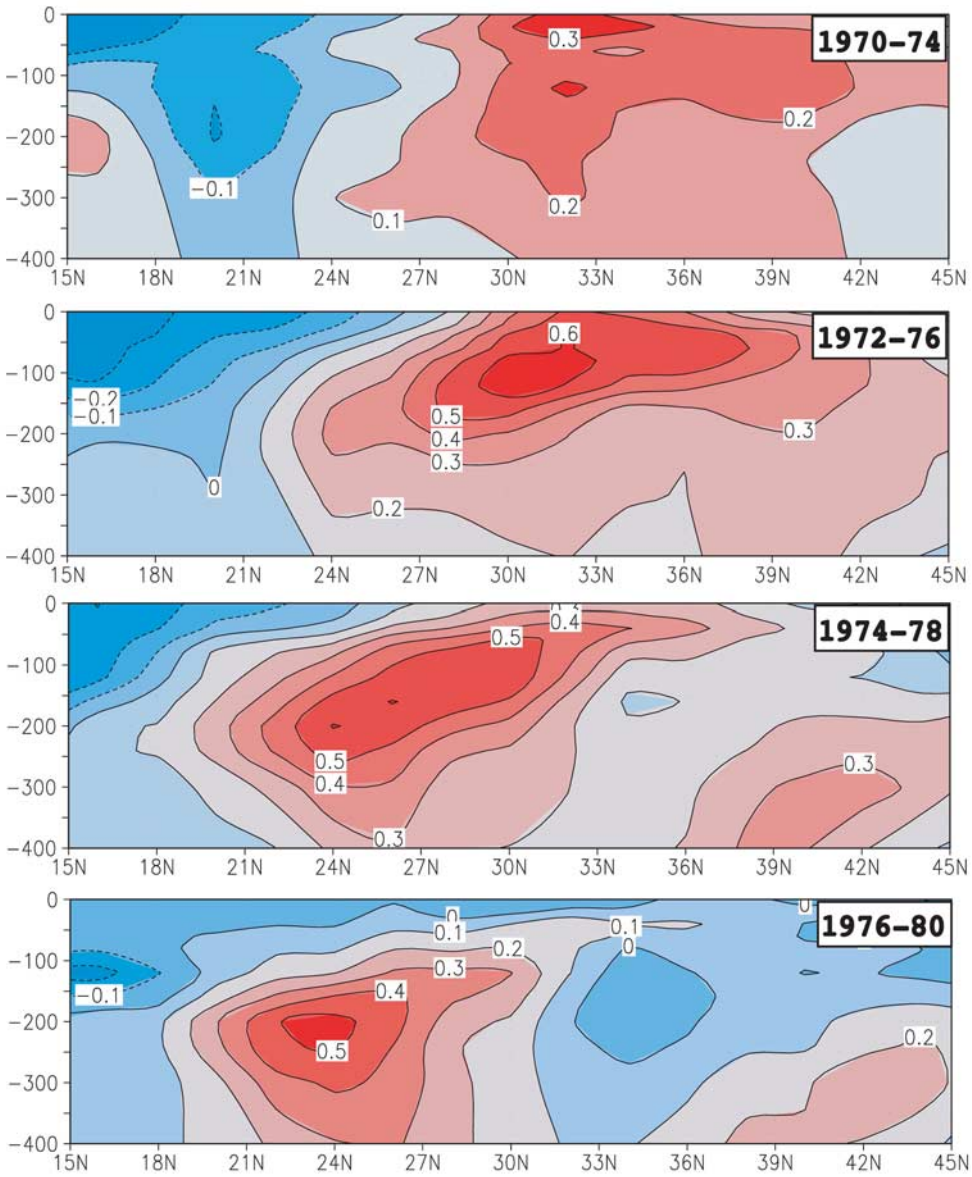

Figure 4. Annual oceanic temperature anomalies as a function of depth and latitude for the longitude band 170°–145°W from 1970 to 1980. The depth range is from the surface to the depth of 400 m. Positive values are indicated by red with solid line, and negative values are indicated by blue with dashed line. A warm anomaly associated with the Pacific decadal climate shift is seen to subduct from the midlatitude toward lower latitudes. Adapted from *Deser et al.* [1996]. Reprinted with permission courtesy of the American Meteorological Society.

about 30°N to 30°S and includes equatorward flow by the surface trade winds, ascent near the equator, poleward flow in the upper troposphere, and descent in the subtropics (Figure 1). Many aspects of the Hadley cell, including its meridional extent, the total poleward heat flux, and the latitude of the upper level jet can be understood from the modeling study of *Held and Hou* [1980]. In their two-layer model, friction is applied only in the lower layer, so air in the upper level conserves angular momentum. As air moves poleward in the upper level, the westerlies (eastward directed winds) increase in order to conserve angular momentum, which leads to "the subtropical jet" at the outer limits of the cell. The upper level winds are also in thermal wind balance; that is, they are directly related to the meridional temperature (θ_M) gradient. The circulation is driven by the difference between θ_M and a specified "radiative equilibrium" temperature (θ_E) of a motionless atmosphere. Where $\theta_E > \theta_M$, there is net heating and vice versa. The steady solution requires that this heating and cooling exactly balance, which sets the extent and strength of the Hadley cell. The model can be extended by including the effects of latent heat release in tropical precipitation and by shifting the mean meridional temperature gradient with the seasons, which results in a much stronger cell in the winter hemisphere [*Lindzen and Hou*, 1988; *James*, 2003; *Cook*, 2004].

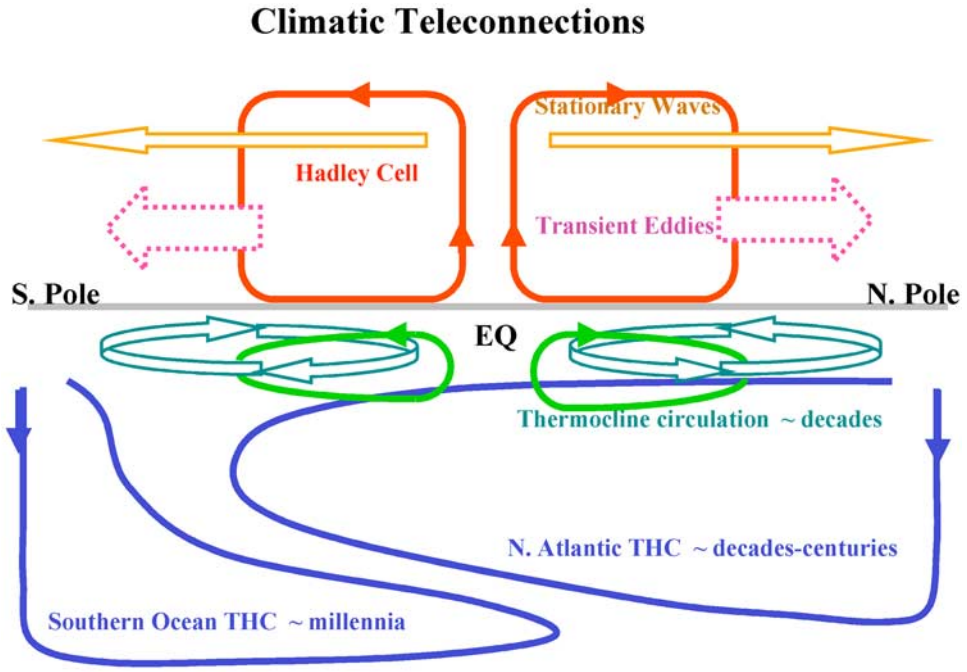

Figure 5. Schematic for the major branches of climatic teleconnections in the atmosphere and ocean. The atmospheric teleconnections occur at fast timescales, usually shorter than a month (not marked). The oceanic teleconnections occur at a wide range of timescales as marked.

[12] In his seminal papers on ENSO-induced atmospheric anomalies, *Bjerknes* [1966, 1969] proposed that enhanced rainfall over the anomalously warm SSTs in the tropical Pacific would intensify the local Hadley circulation, thereby influencing the winds over the North Pacific Ocean during winter. During El Niño events, which are connected over the equatorial Pacific via an eastward displacement of the Walker cell with anomalous easterlies (westerlies) in the upper (lower) troposphere over the equatorial Pacific [e.g., *Wang*, 2003], the local Hadley cell increases (decreases) in the east (west) Pacific. The zonal mean response to ENSO is complex: There is an increase in the strength of the summer Hadley cell [*Oort and Yieneger*, 1996]; a second overturning cell forms that opposes the mean Hadley circulation between 15°N and 30°N [*Waliser et al.*, 1999; *Quan et al.*, 2004]; and the response is nonlinear; that is, the circulation between 15°N and 15°S is much stronger during El Niño than La Niña events (our Figure 6) [*Quan et al.*, 2004].

2.1.2. Eddy-Driven Circulation

[13] Weaker meridional circulations, termed Ferrel cells, flow in the opposite direction to the Hadley cell between approximately 30° and 60° latitude of both hemispheres (Figure 1). They are thermally indirect as they transport energy from cold to warm areas. The Ferrel cells are a byproduct of midlatitude storms (eddies), which are responsible for the majority of the poleward energy transport outside the tropics. The storms derive their energy from the strong meridional temperature gradient, or baroclinicity, in midlatitudes. The net effect of baroclinically unstable eddies over their life cycle is to transport heat and westward momentum poleward, as can be diagnosed by the Eliassen and Palm flux [e.g., *Edmon et al.*, 1980]. This westward momentum slows the winds on the poleward flank of the jet. Eddies also generate upper tropospheric waves that mainly propagate equatorward and then break, decelerating the zonal mean flow in the subtropics [*Randel and Held*, 1991]. Thus eddies maintain the position of the extratropical jet stream by reducing the westerlies on either side of the jet/storm track axis. In turn, the structure of the jet influences the propagation characteristics of eddies including where their momentum is deposited [*Branstator*, 1995], and eddy mean flow can lead to zonally coherent anomalies.

[14] The leading pattern of variability of the extratropical circulation in both hemispheres, as identified by empirical orthogonal function (EOF) analysis, is characterized by zonally symmetric or "annular" structures, with geopotential height perturbations of opposing signs in the polar cap region and in the surrounding zonal ring near 45° latitude with centers over the North Atlantic and Pacific oceans. It is unclear whether the northern annular mode, also termed the Arctic Oscillation (AO) [*Thompson and Wallace*, 1998], is independent from the NAO [e.g., *Hurrell et al.*, 2003], since anomalies over the Pacific often vary independently from those over the Atlantic [*Deser*, 2000; *Ambaum et al.*, 2001]. The structure of the annular modes may partly be an artifact of the EOF analysis methods used to obtain them [*Richman*, 1986; *Dommonget and Latif*, 2002], and the extent to which the AO is a true physical mode of the climate system remains unclear.

[15] The southern annular mode (SAM) has also been referred to as the high-latitude mode [*Karoly*, 1990] and the Antarctic Oscillation [*Gong and Wang*, 1999; *Thompson and Wallace*, 2000]. Annular modes appear to be generated by wave–mean flow interactions in the extratropical circulation, including momentum fluxes from both traveling storms and stationary waves [e.g., *Karoly*, 1990; *Hartmann and Lo*,

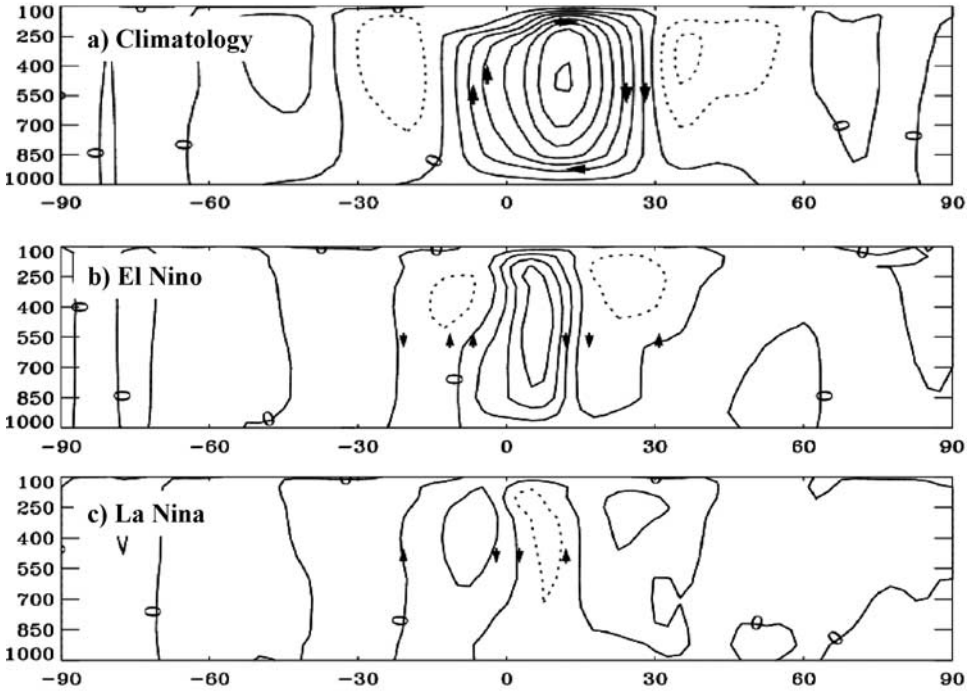

Figure 6. (a) Climatology and anomalous zonal mean meridional stream function during December–January–February (DJF) based on composite averages of (b) El Niño and (c) La Niña events obtained from NCEP reanalysis for the years between 1950 and 2002. Counter interval is 4×10^9 kg s^{-1}. From *Quan et al.* [2004, Figure 3–4], with kind permission from Springer Science and Business Media.

1998; *DeWeaver and Nigam*, 2000a, 2000b; *Robinson*, 2000; *Limpasuvan and Hartmann*, 1999, 2000; *Lorenz and Hartmann*, 2001, 2003]. The annular modes also appear to be influenced by downward coupling between the stratosphere and troposphere [e.g., *Baldwin and Dunkerton*, 1999, 2001; *Black*, 2002; *Perlwitz and Harnik*, 2004].

[16] Eddy–mean flow interactions may lead to connections between zonal anomalies in the tropics and extratropics. During the 1- to 2-week period following the peak amplitude in the extratropical annular modes, there is less wave breaking at tropical latitudes, and the upper tropical troposphere experiences anomalous eastward forcing [*Thompson and Lorenz*, 2004]. Extratropical zonally symmetric anomalies may also involve both overturning circulations and eddy processes. *Chang* [1995, 1998] and *Seager et al.* [2003] found that ENSO-driven changes in the Hadley cell strength alter the subtropical jets, and then transient cyclones propagate in an altered mean zonal flow resulting in changes in eddy momentum fluxes. These fluxes apply a westerly (easterly) force from 30° to 45° (45° to 60°) impacting the jet streams in both hemispheres.

2.2. Zonally Asymmetric Teleconnections

2.2.1. Teleconnection Patterns

[17] More than a dozen teleconnection patterns have been identified in the Northern Hemisphere using correlations and a number of pattern identification techniques, such as EOFs, rotated EOFs, singular value decomposition, and cluster analysis [e.g., *Wallace and Gutzler*, 1981; *Mo and Livezey*, 1986; *Barnston and Livezey*, 1987; *Nigam*, 2003; *Cassou et al.*, 2004]. These include north-south dipole patterns, such as the NAO and west Pacific (WP) patterns, and wave-like patterns, such as the PNA and the tropical–Northern Hemisphere (TNH) pattern, which are most prominent in winter (Figure 7). The Pacific Japan (PJ) pattern, which consists of a north-south dipole with atmospheric anomalies centered at about 20°N, 35°N, and 50°N between 100°E and 160°W, appears to be associated with convection near the Philippines and meridional displacement of the jet over the Northern Hemisphere in summer [*Nitta*, 1987; *Kosaka and Nakamura*, 2007]. Many of these patterns, such as the NAO and WP, occur in atmospheric general circulation models (AGCMs) with climatological SSTs specified as boundary conditions, indicating that they are primarily generated by internal atmospheric processes. Others, such as the TNH pattern, appear to be due to tropical forcing associated with ENSO during winter, while the PNA and PJ patterns appear to be both intrinsic to the atmosphere and forced by ENSO. In addition to the Antarctic Oscillation, teleconnections in the Southern Hemisphere include the Pacific–South America patterns, a pair of wave-like patterns with three centers of action that extend across the Pacific from New Zealand to the southern tip of Argentina [e.g., *Robertson and Mechoso*, 2003], and a zonal wave number 3 pattern over the Southern Ocean [*Mo and White*, 1985; *Raphael* 2004]. For a more in depth discussion

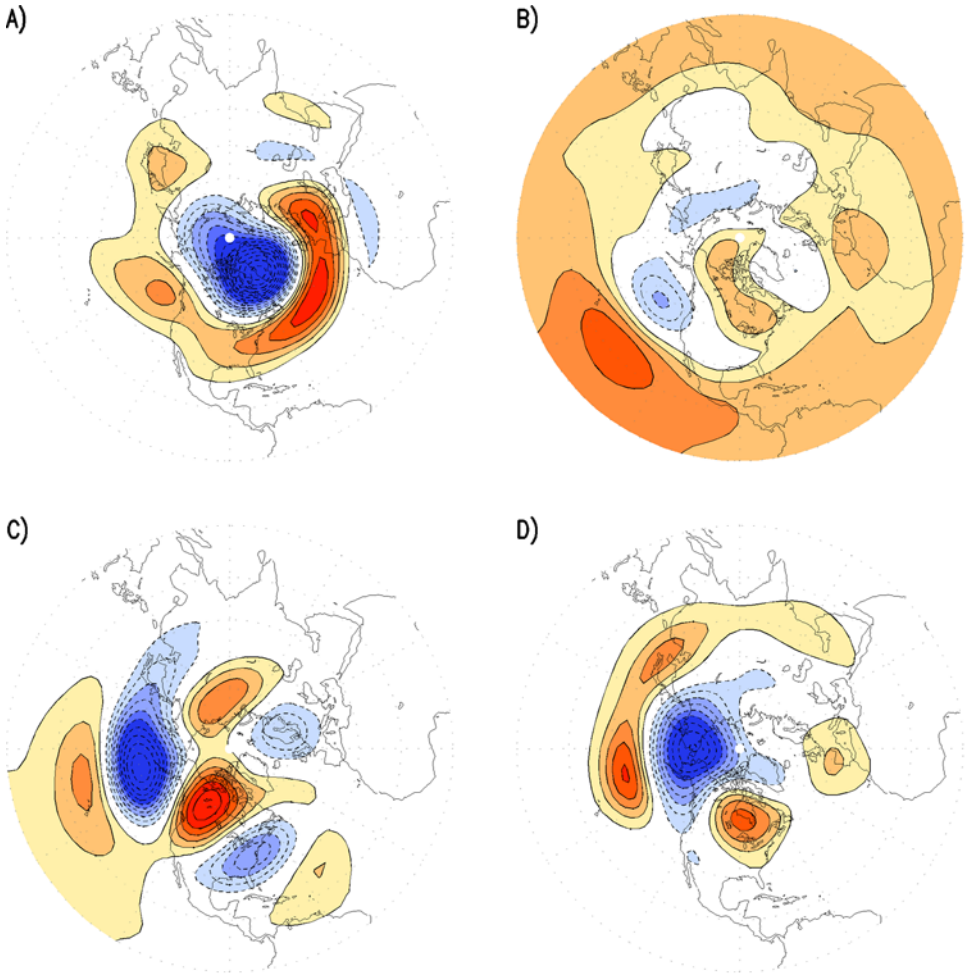

Figure 7. Leading teleconnection patterns of height variability at 200 mb: (a) North Atlantic Oscillation (NAO or AO), (b) ENSO-driven tropical Northern Hemisphere (TNH), (c) Pacific North American (PNA), and (d) west Pacific (WP). The patterns are based on monthly fluctuations during DJF over 30°S–90°N for the period 1958–1988. The patterns, obtained from rotated principal component analyses, are orthogonal in time but not in space. The contour interval is 10 m, where the zero contour is suppressed. Patterns in Figures 7a–7d explain 15.1%, 13.3%, 11.9%, and 8.7%, respectively, of the domain-averaged variance. Reprinted from *Nigam* [2003], with permission from Elsevier.

of teleconnections and their dynamics, see *Glantz et al.* [1991], *Trenberth et al.* [1998], and *Nigam* [2003].

2.2.2. Teleconnection Dynamics

2.2.2.1. Internal Causes for Teleconnection Patterns

[18] Several of the meridional dipole teleconnection patterns are located downstream and poleward of the mean position of the jet stream and extratropical storm tracks. Like the zonally symmetric anomalies these patterns appear to result from eddy–jet stream interactions, as indicated by positive feedbacks between the rapidly passing and the relatively stationary low-frequency variability [e.g., *Hoskins et al.*, 1983; *Lau*, 1988; *Lau and Nath*, 1994; *Branstator*, 1995]. In addition to drawing their energy from baroclinic instability, atmospheric perturbations can grow from barotropic instability associated with horizontal gradients in the wind. *Simmons et al.* [1983] found that barotropic perturbations could intensify from the longitudinal gradients in the jet exit regions and come to resemble teleconnection patterns over time, but these disturbances appear to develop too slowly to overcome dissipative effects in the atmosphere [*Borges and Sardeshmukh*, 1995].

[19] Many theories for teleconnection patterns involve Rossby or planetary waves, where the wave propagation depends on the background wind field (see section A1). Regions of strong zonal wind shear, which occur in the vicinity of the jet stream, strongly refract, or bend, waves of a certain scale confining them to the vicinity of the jet [*Branstator*, 1983; *Hoskins and Ambrizzi*, 1993]. As a result, chains of highs and lows with maximum amplitude in the upper troposphere are centered near the core of the subtropical jet during winter. These patterns can extend completely around the globe, and during this circumglobal phase include a north-south dipole over the Atlantic that closely resembles the NAO [*Branstator*, 2002]. The propagation of energy associated with stationary Rossby waves also impacts teleconnections outside of the waveguide linking variations in the Aleutian and Icelandic lows in late winter [*Honda et al.*, 2001, 2005].

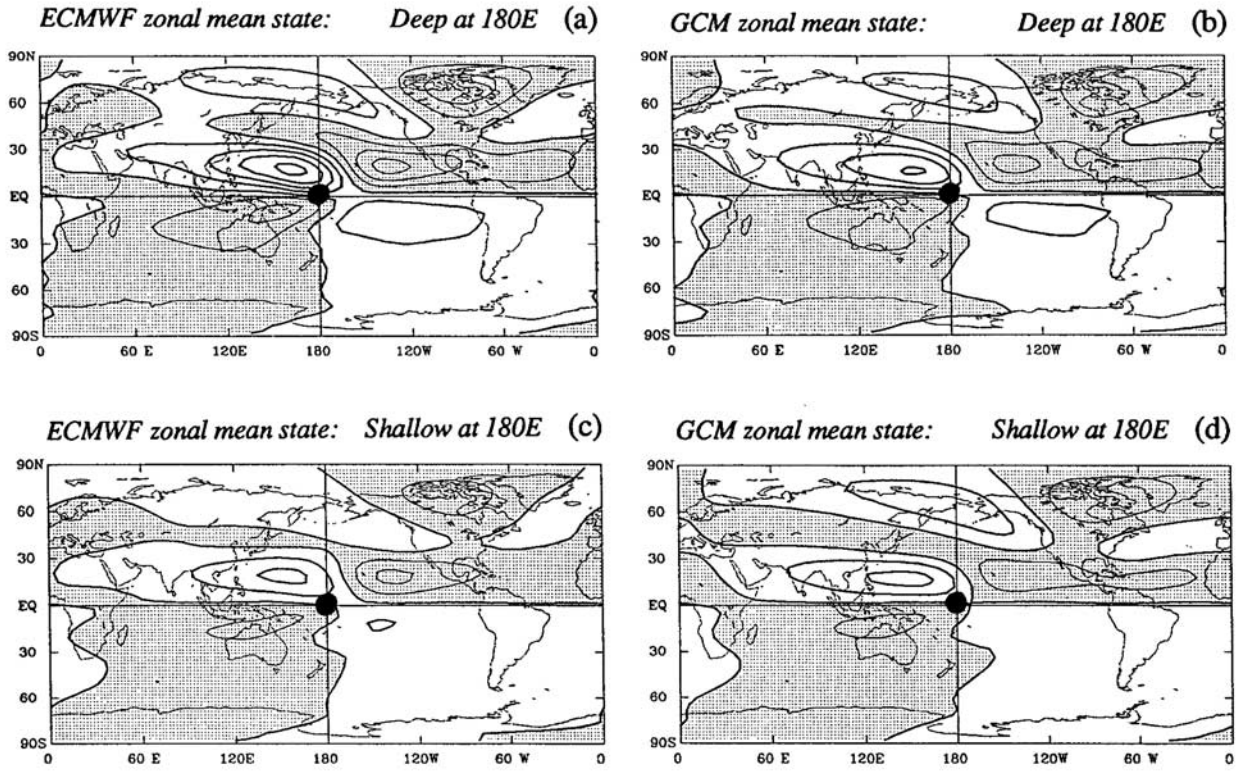

Figure 8. Steady state stream function response to upper troposphere "deep" heat sources located along the equator that peak in the mid-to-upper troposphere. The forcing is imposed at (a) 180° on a zonally uniform basic state (that includes zonal and meridional winds), while the forcing is centered at (b) 180°E, (c) 180°, and (d) 180°W on a "wavy" background flow where the winds are a function of longitude. The contour interval is 4×10^6 m^2 s^{-1}; negative values are shaded. The location of maximum heating is denoted by circles. The winds are parallel to the contour lines, and positive (negative) extremes are associated with anomalous clockwise (counterclockwise) flows. The climatological winds used for the basic state are based on European Centre for Medium-Range Weather Forecasting. Adapted from *Ting and Sardeshmukh* [1993]. Reprinted with permission courtesy of the American Meteorological Society.

2.2.2.2. Tropically Forced (SST Driven) Variability

[20] In the early 1980s the combination of research on teleconnection patterns [*Wallace and Gutzler*, 1981], the atmospheric circulation anomalies associated with convective precipitation and SST anomalies in the tropical Pacific [*Gill*, 1980; *Horel and Wallace*, 1981], and Rossby wave dispersion [*Hoskins and Karoly*, 1981] led to a much improved understanding of the atmospheric response to El Niño. During El Niño events, enhanced precipitation and midlevel heat release occur above the anomalously warm SSTs in the central equatorial Pacific. The seminal work of *Gill* [1980] showed that the response of the tropical circulation to this heating includes a pair of low level (upper level) cyclones (anticyclones) located poleward and to the west of the heat source and low pressure that extends well to the east of the heating along the equator. The signal along the equator is associated with a Kelvin wave, while the off-equatorial circulations are associated with stationary Rossby waves. Owing to nonlinear advection and the time dependence of vorticity sources the upper level anticyclones associated with the Rossby waves in observations and AGCM experiments are located east of those in the Gill solution [*Sardeshmukh and Hoskins*, 1985] at about the same longitude as the SST/air temperature anomalies (Figure 3).

[21] The ENSO-related tropical forcing also generates Rossby waves that propagate into the extratropics (see section A1). For the basic theory, which utilizes the shallow water vorticity equation on the sphere linearized about the zonal mean zonal wind (U), the wave energy follows great circle routes, initially extending poleward and eastward, refracting (turning) away from the pole and returning to the tropics [see *Hoskins and Karoly*, 1981; *Trenberth et al.*, 1998]. The response to subtropical forcing in this framework resembles observations in terms of the spatial scale, the broad trajectory of the anomalies, and the time it takes to fully establish the teleconnection patterns. However, the waves are unable to propagate through easterly winds and through regions where the meridional wind shear changes rapidly with latitude. The response to forcing near the equator more closely resembles observed teleconnection patterns when the circulation is linearized about more realistic flows (Figure 8a), as discussed below. The approximately 2–6 weeks predicted by the basic Rossby wave theory to establish teleconnection patterns has been confirmed in AGCM simulations (Figure 9).

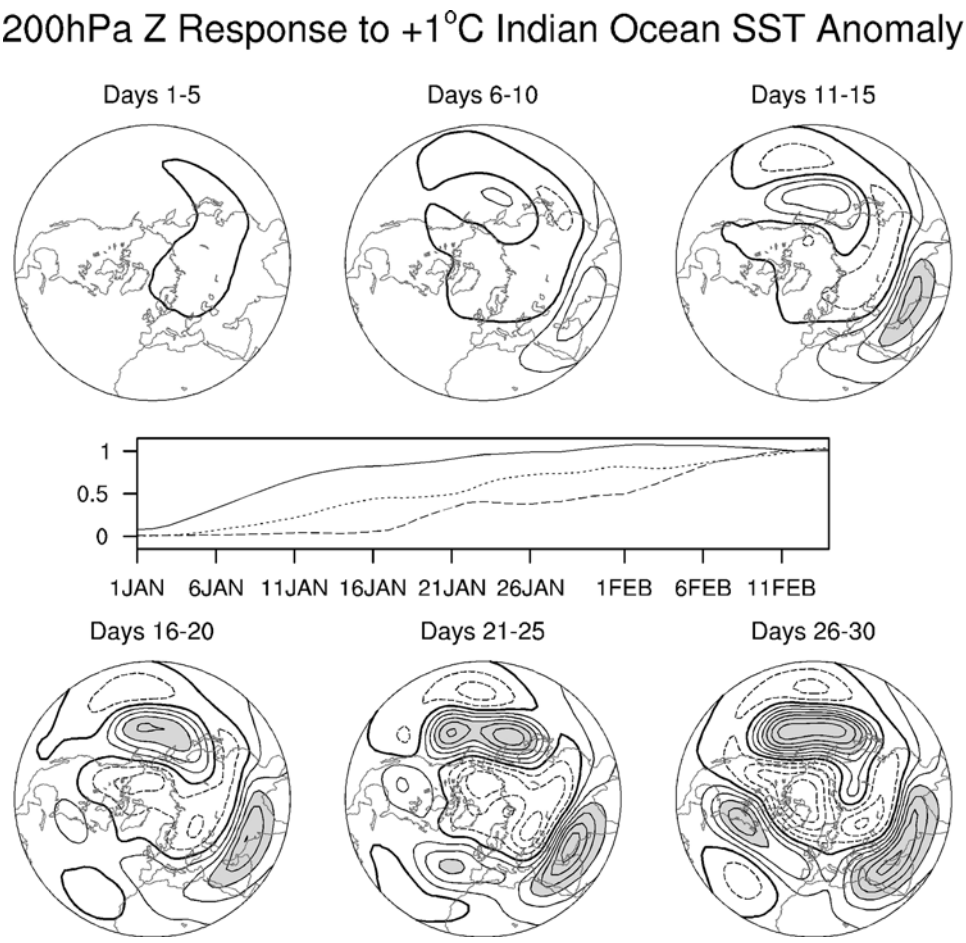

Figure 9. Transient response of an atmospheric general circulation model (GCM) (the National Center for Atmospheric Research (NCAR) Community Climate Model, version 3) to a +1°C warming of the tropical Indian Ocean. Shown are consecutive 5-day averaged anomalies of 200 mb height through days 26–30 (bottom, right). The center graph shows time series (days 1–45) of 200 mb heights (m) averaged over areas of developing anticyclones: South Asia (10°N–30°N, 40°E–90°E; solid curve), North Pacific (40°N–50°N, 150°E–180°; dotted curve), and North Atlantic (40°N–50°N, 45°W–15°W; dashed curve). The time series anomalies are standardized by the response at 41–45 days, when the model reaches equilibrium. The contour increment is 15 m, negative values are dashed, and responses exceeding +45 m are shaded. Reprinted from *Hoerling et al.* [2004, Figure 10], with kind permission from Springer Science and Business Media.

[22] Several aspects of the observed teleconnections to the extratropics cannot be explained by the basic Rossby wave theory, including the following: (1) The atmospheric anomalies are baroclinic in the tropics, but by the time they reach the extratropics, they have an equivalent barotropic structure (where the anomaly pattern remains the same through the troposphere but the amplitude changes (usually increases) with height). (2) Wave trains extend into the extratropics even when there is a critical line ($U = 0$) poleward of the forcing where linear theory indicates that the Rossby waves should be dissipated or reflected. (3) Wave trains have preferred locations even when the initial heat source moves geographically. (4) Nonlinear interactions may impact teleconnections and generate differences between the response to El Niño and La Niña conditions. These deficiencies can be ameliorated by a combination of factors.

[23] 1. Given that the climatological or background flow is not strictly zonal nor uniform with height or longitude, Rossby waves can propagate through longitudinal/vertically confined regions of westerlies, "westerly ducts" [*Webster and Holton*, 1982; *Branstator*, 1983; *Kiladis and Weickmann*, 1992], and meridional flow can also enable the propagation of Rossby waves through regions of easterly winds [*Schneider and Watterson*, 1984; *Ting and Sardeshmukh*, 1993] (Figure 8a). The climatological flow also varies with the seasonal cycle, which changes the shape of the Rossby waveguide and the regions where convection is most effective in forcing extratropical circulation anomalies. [*Newman and Sardeshmukh*, 1998].

[24] 2. The inclusion of the time-averaged vertical shear can also convert baroclinic into barotropic disturbances, where the baroclinic modes are equatorially trapped, while the barotropic modes can more readily propagate to midlat-

itudes [*Lim and Chang*, 1986; *Kasahara and Silva Dias*, 1986; *Wang and Xie*, 1996]. *Kosaka and Nakamura* [2007] invoked a superposition of barotropic and baroclinic modes to explain the occurrence of the PJ pattern in summer.

[25] 3. The initial wave models only considered the Rossby wave forcing due to vortex stretching, i.e., advection of the mean vorticity by the anomalous divergence, but the advection of vorticity by the anomalous divergent component of the flow is also an important Rossby wave source [*Sardeshmukh and Hoskins*, 1988]. Divergent flow anomalies in regions of strong vorticity gradients can effectively generate Rossby waves even when they are far from the heat source that induced them.

[26] 4. There are multiple SST and heat sources/sinks during ENSO events [*Barsugli and Sardeshmukh*, 2002; *DeWeaver and Nigam*, 2004]. For example, SST anomalies, beyond the traditional ENSO region, such as those west of the date line in the tropical Pacific, appear to be very affective at generating the PNA pattern [*Barsugli and Sardeshmukh*, 2002]. Convergence in the subtropical Pacific is an important wave source [*Held and Kang*, 1987; *Rasmusson and Mo*, 1993], while the Rossby wave response to anomalous heating in the Indian Ocean tends to oppose the response from the Pacific over the PNA region (Figure 9) [*Ting and Held*, 1990; H. Annamalai and H. Okajima, Role of the Indian Ocean SST on Northern Hemisphere circulation during El Niño years, submitted to *Journal of Climate*, 2005, hereinafter referred to as Annamalai and Okajima, submitted manuscript, 2005].

[27] 5. Changes in the midlatitude storm tracks during El Niño events alter the eddy momentum fluxes thereby influencing the amplitude and structure of the wave trains initiated by tropical heating. [*Kok and Opsteegh*, 1985; *Held et al.*, 1989; *Hoerling and Ting*, 1994].

[28] 6. Since convection in the tropical Pacific depends on the mean SST, i.e., precipitation is enhanced above ~27.5°C [*Graham and Barnett*, 1987; *Waliser and Graham*, 1993], there is more warm water above this threshold in the central and eastern Pacific and thus enhanced diabatic heating during El Niño events compared to La Niña events. *Hoerling et al.* [1997, 2001b] found that this nonlinearity in the heating influences the extratropical atmospheric teleconnections, but *DeWeaver and Nigam* [2002] attributed much of the extratropical asymmetry to decadal differences in the base state rather than to differences between warm and cold events. Nonlinearities can also impact the response to ENSO as a result of the forcing first modifying the extratropical circulation in essence creating a different base state. Nonlinearity of the midlatitude dynamics can also give rise to asymmetry between the response to tropical heating and an equal and opposite cooling [*Hall and Derome*, 2000]. While the PNA pattern is primarily a direct response to the tropical forcing, the sensitivity of the response to the base state was a key factor in the asymmetrical response to El Niño versus La Niña over the North Atlantic [*Sardeshmukh et al.*, 2000; *Lin and Derome*, 2004].

[29] While most studies have focused on ENSO teleconnections to the Northern Hemisphere in winter, there is clearly a strong ENSO signature in the Southern Hemisphere (Figure 3) [*Van Loon and Shea*, 1987; *Kidson* 1988; *Cook*, 2001] and in the North Pacific in boreal summer [*Nitta*, 1987; *Lau and Peno*, 1992; *Chen and Yen*, 1993; *Alexander et al.*, 2004b; *Kosaka and Nakamura*, 2007]. The latter exists despite strong easterlies throughout the tropics in boreal summer, and thus processes such as anomalous convection and vorticity advection in the subtropics and interaction with eddies (as discussed above) are likely to be vital in establishing the northern summer pattern.

[30] Recent studies also indicate that SST anomalies in other tropical basins can influence the extratropical circulation. *Hoerling et al.* [2001a, 2004] and *Hoerling and Kumar* [2003] (Figure 9) indicate that some of the trend in the North Atlantic Oscillation results from long-term warming over the Indian Ocean. An east-west SST dipole in the equatorial Indian Ocean, due to both local air-sea interaction and forcing from ENSO [e.g., *Saji et al.*, 1999; *Saji and Yamagata*, 2003; *Lau and Nath*, 2004; *Shinoda et al.*, 2004], may influence the Asian and Australian monsoons and the broader atmospheric circulation [*Saji and Yamagata*, 2003]. In addition, SST anomalies in the southeast Indian Ocean that result from the ocean's dynamical response to ENSO [*Xie et al.*, 2002] force an atmospheric Rossby wave train response that counteracts the initial ENSO forcing (Annamalai and Okajima, submitted manuscript, 2005). In the tropical Atlantic, SST anomalies alter the location of the ITCZ, and the resulting changes in heating generate Rossby waves that propagate to the extratropics [*Sutton et al.*, 2000; *Drevillon et al.*, 2003].

2.2.2.3. Middle- and High-Latitude Boundary Forcing

[31] While extratropical ocean and ice anomalies influence the atmospheric circulation, most studies have found this effect to be modest compared to internal atmospheric variability and the response to tropical SST anomalies [see *Kushnir et al.*, 2002, and references therein]. The initial response to surface thermal forcing tends to be fairly localized and baroclinic with a low-level trough located slightly downstream (generally to the east) of the forcing, such that the heating is balanced by horizontal advection [*Hoskins and Karoly*, 1981; *Hall et al.*, 2001]. Depending on the relationship between the anomalous heating and the climatological flow, the thermal response can interact with the storm tracks. The resulting eddy momentum fluxes drive a large-scale equivalent barotropic response [*Peng and Whitaker*, 1999], which often resembles the internal modes of atmospheric variability [*Peng and Robinson*, 2001; *Alexander et al.*, 2004a; *Deser et al.*, 2004a]. Thus changes in extratropical SST and sea ice can have some influence on the probability distributions of extratropical teleconnection patterns.

3. OCEANIC TELECONNECTIONS

[32] The global ocean stratification is determined predominantly by ocean circulation, because solar radiation is trapped within about 50 m of the surface [*Rochford et al.*, 2001; *Murtugudde et al.*, 2002]. This differs fundamentally

from the atmosphere, whose stratification is determined at the first order by local radiative-convective equilibrium. Historically, the extremely cold water measured at depth in the tropical Atlantic [*Ellis*, 1751] has prompted speculation that cold low-latitude subsurface water must be sustained by cold currents originating from polar regions [*Rumford*, 1800]. Noting the shallowing of the tropical thermocline toward the equator, *Lenz* [1845] further inferred the presence of a pair of symmetric equatorial upwelling thermohaline cells, one in each hemisphere (see *Warren* [1981] for a historical review). In spite of the long-term recognition of some qualitative aspects of the ocean circulation, direct measurements of the circulation remain poor even today, especially for the slow abyssal flow and the THC. Nevertheless, present observations appear to provide a reasonable estimate of the gross features of world ocean circulation [*Macdonald and Wunsch*, 1996]. Over the last 2 decades, improved data, models, and theory have led to substantial progress in our understanding of both the deep THC and the shallow wind-driven circulation.

3.1. Deep Thermohaline Teleconnection

3.1.1. Thermohaline Circulation

[33] Today the deepwater mass of the world ocean is formed by deep convection mainly from the northern part of the North Atlantic (Greenland-Iceland-Norwegian seas) and around the Antarctic (mainly the Weddell Sea) as the North Atlantic Deep Water (NADW) and Antarctic Bottom Water (AABW), respectively [*Warren*, 1981]. The NADW flows southward at the depth of 2000–3000 m with a transport of about 15–20 Sv (1 Sv = 10^6 m^3 s^{-1}); most of the water crosses the equator and upwells in the South Atlantic and Southern Ocean (Figure 2c). The AABW, which has a transport substantially weaker than the NADW, spreads northward on the ocean floor against the South America and the Mid-Atlantic Ridge. The abyssal flows are carried mainly in the deep western boundary currents (DWBC), which can be inferred even from early hydrographic observations [*Defant*, 1941]. The DWBC and the west-east asymmetry of the abyssal flow can be understood from the conservation of potential vorticity on a rotating sphere [*Stommel*, 1958; *Stommel and Arons*, 1960]. This western boundary intensification is a general feature to the ocean circulation in both the upper (see section 3.2) and deep oceans. In essence, this west-east asymmetry of the flow pattern is due to the asymmetric nature of the Rossby wave: A western boundary only generates short Rossby waves, whose slowly eastward propagating kinetic energy is trapped by mixing effects near the western boundary to form an intensive current [*Pedlosky*, 1987a] (section A2). This strong west-east asymmetry, in conjunction with the meridional overturning circulation, creates an intrinsically three-dimensional THC. In this type of three-dimensional flow the trajectories of water parcels can be extremely complex and even chaotic [*Yang and Liu*, 1997]. Therefore any simple picture of the global THC in terms of water parcel trajectories and transport, such as the "conveyor belt" [*Broecker and Denton*, 1989], should be treated only as a schematic depiction of the circulation.

[34] Traditionally, the studies of THC emphasized the competitive driving of high-latitude heat and freshwater fluxes [*Stommel*, 1961; *Marotzke et al.*, 1988]. The colder temperature at high latitudes favors a thermal circulation that sinks at high latitudes, while the higher salinity at low latitudes favors a haline circulation that sinks at low latitude. Currently, the temperature effect dominates, resulting in a THC that sinks at high latitudes. The competition between the thermal and haline forcing also results in positive feedbacks that may lead to abrupt changes [*Bryan*, 1986] and internal variability [*Weaver et al.*, 1994] in the THC. It has been recognized recently, however, that the total global water mass formation rate and overturning rate is limited not by the efficiency of high-latitude convective mixing but rather by the pole-equator density difference and the ocean's ability to warm the upwelling deep water [*Bryan*, 1987; *Marotzke and Scott*, 1999]. The warming rate of the upwelling water depends critically on the oceanic diapycnal mixing, which converts the cold deep water to warm surface water and therefore resupplies the potential energy removed in the interior by the overturning circulation [*Huang*, 1999]. It is recognized that the energy for the small-scale internal mixing is contributed mainly by the surface wind and internal tide [*Munk and Wunsch*, 1998; *Paparella and Young*, 2002; *Wunsch and Ferrari*, 2004; *Wang and Huang*, 2005], but the detailed process of the energy transfer remains unclear. In this view, rather than being a heat engine driven by buoyancy forcing like the atmospheric Hadley cell, the oceanic THC is an indirect circulation that is largely driven by the mechanical forcing of tide and wind. This is an area of intensive recent research, and its implication for climate teleconnection remains to be explored.

3.1.2. Pole-Pole Circulation and Interhemispheric Teleconnection

[35] The present North Atlantic THC is characterized by a strong equatorial asymmetry, with the transport of the NADW much stronger than that of the AABW. Consequently, the overturning circulation in the Atlantic is dominated by a deep southward flow across the equator and a surface return flow (Figure 2c). This dominance of the asymmetric THC in the Atlantic results in a northward oceanic heat transport all the way from the South Atlantic to the North Atlantic [*Hastenrath*, 1982]. This observed asymmetry has important climate implications. Earlier studies on THC use the pole-equator single-hemisphere model, in which the THC is generated by the pole-equator density contrast [*Stommel*, 1961]. Since the pole-equator density contrast is largely symmetric about the equator, the resulting THC is largely symmetric about the equator too. In this symmetric view the salinity forcing acts to oppose the temperature forcing and always provides a positive feedback to THC instability [*Scott et al.*, 1999]. However, the actual THC is better characterized by a pole-pole interhemispheric model [*Rooth*, 1982; *Bryan*, 1986]. In this inter-

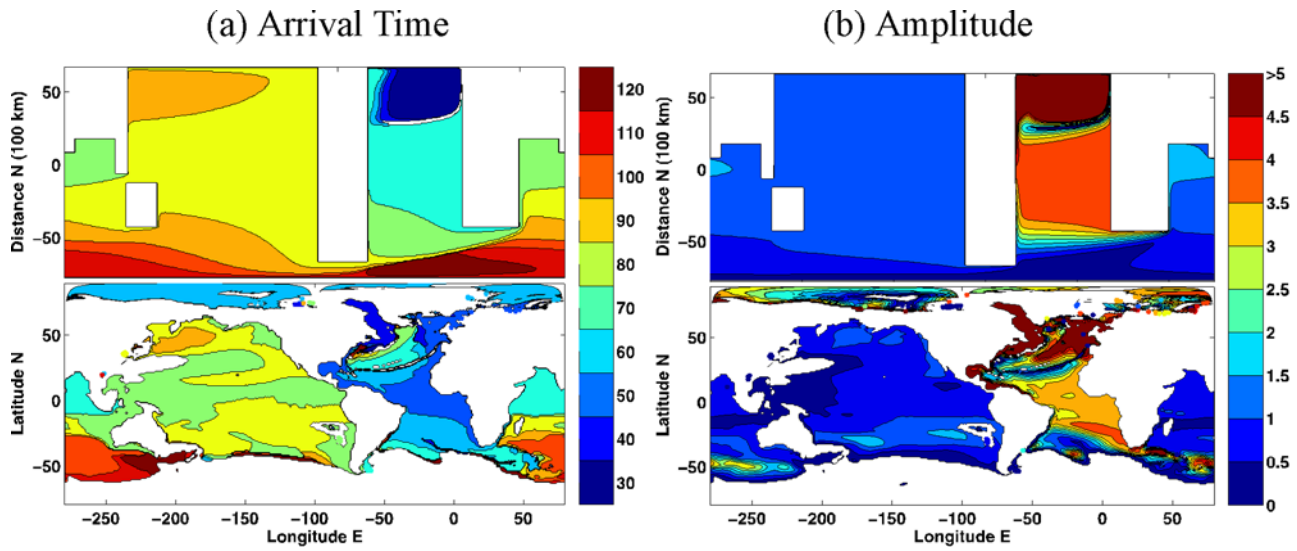

Figure 10. (a) Time of arrival (years) and (b) amplitude (centimeters) of the first maximum in sea surface height in response to a change in the northern North Atlantic. The freshwater forcing is a "switch-on" sinusoid with a period of 100 years near the region of Greenland. (top) Plots are from a reduced gravity model for a simplified world geometry. (bottom) Plots are from a general oceanic circulation model with realistic world ocean topography. Both models show qualitatively similar results, with the signal spreading first in the Atlantic and then in the Indian Ocean and finally in the Pacific in about 100 years. The amplitude in the Pacific, however, is several times smaller than that in the Atlantic. The variability in the simple model is caused almost entirely by Kelvin and Rossby waves. The similar response in the ocean general circulation model suggests that the same process also largely holds in the complex ocean model. Adapted from *Cessi et al.* [2004].

hemispheric view the strength of the North Atlantic THC is proportional to the column average density difference between the Southern Ocean and the North Atlantic [*Hughes and Weaver*, 1994; *Rahmstorf*, 1996]. Indeed, warm waters are mostly trapped in the upper ocean and therefore have little direct impact on abyssal water masses and, in turn, the global THC. On the other hand, a slight asymmetry between the density forcings in the two poles can result in a dramatically asymmetric deep THC circulation [*Klinger and Marotzke*, 1999]. Furthermore, the interhemispheric THC is much more sensitive to perturbations than the symmetric THC, because the climatological density contrast is about 1 order smaller for the pole-pole than for the pole-equator. Therefore the actual THC is strongly related to interhemispheric teleconnections.

[36] The Southern Ocean is unique in determining the interhemispheric THC. The freshwater forcing on the Southern Ocean is much more important than that on the North Atlantic in determining the final equilibrium of the interhemispheric THC. Theoretical studies have shown that the final equilibrium of the pole-pole THC is determined by the freshwater forcing over the rising branch instead of the sinking branch [*Rooth*, 1982; *Rahmstorf*, 1996; *Scott et al.*, 1999]. Furthermore, the absence of a meridional boundary results in a much longer response time of the global THC to climate forcing over the Southern Ocean than, say, over the North Atlantic. First, oceanic teleconnection across the Southern Ocean is established at a much longer time because of the absence of meridionally propagating Kelvin waves and the deep western boundary current, as will be discussed in section 3.1.3. Instead, heat transport across the Southern Ocean is accomplished mostly by eddy mixing. Second, surface ocean mixing extends into the deep ocean because of the absence of a sharp thermocline. This deep mixing may be facilitated by the wind forcing, which, in the absence of a meridional boundary in the upper half of the Southern Ocean, forces a northward surface Ekman transport, whose returned flow forms an apparent deep overturning Deacon cell in the Southern Ocean (Figure 2a). The dramatically different dynamics and timescales between the Southern Ocean and the North Atlantic may have important implications for interhemispheric climate interactions (see section 4.3).

3.1.3. Thermohaline Adjustment and Ocean Wave Teleconnections

[37] The equilibrium of the world ocean deepwater mass takes thousands of years because of the slow abyssal flow transport and weak mixing [e.g., *Wang et al.*, 1999]. However, the abyssal circulation can adjust rapidly in decades to centuries through the propagation of oceanic waves (Figure 10) [*Kawase*, 1987; *Johnson and Marshall*, 2002]. A deepwater source from the North Atlantic first excites a Kelvin wave that propagates as the first baroclinic mode at a speed of about 3 m s^{-1}. In several months this Kelvin wave propagates southward along the western boundary, propagates eastward along the equator, and then splits poleward along the eastern boundaries toward both hemispheres. The eastern boundary Kelvin waves excite long Rossby waves that propagate westward across the ocean basin (section A2), filling the interior basin with a

weak poleward flow in decades (Figure 10). On the western boundary, short Rossby waves are generated and arrested by local mixing [*Pedlosky*, 1987a], modifying the southward DWBC in the North Atlantic, and establishing a southward DWBC in the South Atlantic. The DWBC also transports mass southward [*Marotzke and Klinger*, 2000]. Eventually, the two DWBCs connect continuously across the equator, establishing an interhemispheric DWBC teleconnection.

[38] The wave propagation can further spread around the world ocean to form a world ocean wave teleconnection (Figure 10). The Kelvin wave on the South Atlantic eastern boundary further propagates around the tip of South Africa into the Indian Ocean and eventually through the Indonesian Throughflow into the Pacific Ocean. These Kelvin waves also excite long Rossby waves that propagate into the interior ocean and eventually establish a global THC conveyor belt [*Broecker and Denton*, 1989]. This wave process represents a global oceanic teleconnection of centennial timescales [*Huang et al.*, 2000; *Cessi et al.*, 2004; *Johnson and Marshall*, 2004], much faster than the millennial advective timescale of the deepwater transport. Although the qualitative feature of this global wave teleconnection is robust, the magnitude of the remote response remains uncertain because of its dependence on diapycnal mixing processes [*Huang et al.*, 2000]. In an ocean general circulation model (OGCM) simulation the remote thermocline change (implied from the sea level change) is about 20% in the Pacific relative to the Atlantic [*Cessi et al.*, 2004]. Nevertheless, this rapid THC adjustment may still be important for our understanding of the role of THC in climate change.

3.2. Shallow Thermocline Teleconnection

3.2.1. Gyre Circulation

[39] It has long been known that the Ekman pumping associated with the wind curl forcing forces a gyre circulation, which consists of a slow interior Sverdrup flow [*Sverdrup*, 1947] and an intensive western boundary return current, such as the Gulf Stream and the Kuroshio extension region [*Stommel*, 1960; *Stommel and Yoshida*, 1972]. This gyre circulation contributes to a significant poleward heat transport in the ocean, especially in the Pacific, where its contribution amounts to about half of the oceanic heat transport [*Hall and Bryden*, 1982; *Bryden et al.*, 1991]. The adjustment of the thermocline circulation is accomplished by planetary Rossby waves (section A2), similar to the abyssal ocean. Unlike the abyssal ocean, however, thermocline adjustment is largely independent of coastal Kelvin waves. This is because the thermocline circulation is driven directly by basin-wide wind forcing, and therefore the Kelvin wave connection around the basin is no longer important (except for circulation along the equator [*Cane and Sarachik*, 1976, 1977; *Philander and Pacanowski*, 1980] or around an island [*Liu et al.*, 1999b]). In the interior ocean the total thermocline circulation is established by the first baroclinic mode of long Rossby waves [*Anderson and Gill*, 1975] (section A2). The stratification structure of the circulation within the thermocline [*Rhines and Young*, 1982; *Luyten et al.*, 1983], on the other hand, is established by higher baroclinic modes of Rossby waves [*Liu*, 1999]. The western boundary intensification is caused by the dissipative energy trapping of short Rossby waves [*Pedlosky*, 1987a] as in the case of DWBC. However, the strong wind-driven interior circulation also enables the onshore Sverdrup flow to trap Rossby wave energy against the western boundary in the incoming flow region [*Charney*, 1955; *Pedlosky*, 1987a]. In the exit region the western boundary current becomes strongly unstable; the unstable waves induce strong mixing of potential vorticity and, in turn, form tight inertial recirculation cells [e.g., *Bryan*, 1963; *Cessi et al.*, 1987].

3.2.2. Subtropical Cell

[40] In the tropical-subtropical region the poleward Ekman flow is returned as an equatorward ventilation of extratropical surface water, forming the STC (Figures 2a–2c top plots). The mass transport of global STCs is comparable with that of the atmospheric Hadley cell [*Held*, 2001]. Associated with the sharp stratification in the tropical-subtropical ocean, the STC contributes significantly to the poleward heat transport in the tropic-subtropical region, especially in the deep tropics where the STC has a heat transport stronger than the Hadley cell [*Held*, 2001]. *Klinger and Marotzke* [2000] estimated a heat transport of about 0.3 PW and 0.1 PW in the Pacific and Atlantic, respectively. Furthermore, subsurface ventilation flow provides an important ocean teleconnection relevant to climate because the water conserves the temperature and other water properties. The equatorward ventilation from the midlatitude has received particular attention because it provides cold source waters to the equatorial undercurrent, which is critical for the maintenance of the equatorial thermocline [*Pedlosky*, 1987b].

[41] We will highlight the major features of the STC here, and readers are referred to *Liu and Philander* [2001] and *Schott et al.* [2004] for more details. The transport of the STC is determined by the trade wind at the tropical-subtropical boundary through its driving of the Ekman flow [*Liu et al.*, 1994; *McCreary and Lu*, 1994]. It should be pointed out, however, that the zonal mean transport (Figure 2) masks two important features of the three-dimensional subtropical-tropical exchange flow. First, the ventilation flow consists of three pathways, which have all been confirmed by tracer and hydrographic observations [*Fine et al.*, 1987; *Johnson and McPhaden*, 1999]. Waters subducted in the central and eastern basins penetrate equatorward through the low-latitude western boundary current pathway and the interior pathway, respectively, while waters subducted in the western basin recirculate back to the extratropics through the poleward western boundary current (Figure 11). Second, the equatorward ventilation is subducted throughout the entire subtropical gyre all the way to the midlatitude, while the zonal mean transport would have implied an equatorward ventilation confined equatorward of 30° where the zonal wind, and, in turn, the poleward Ekman transport, vanishes.

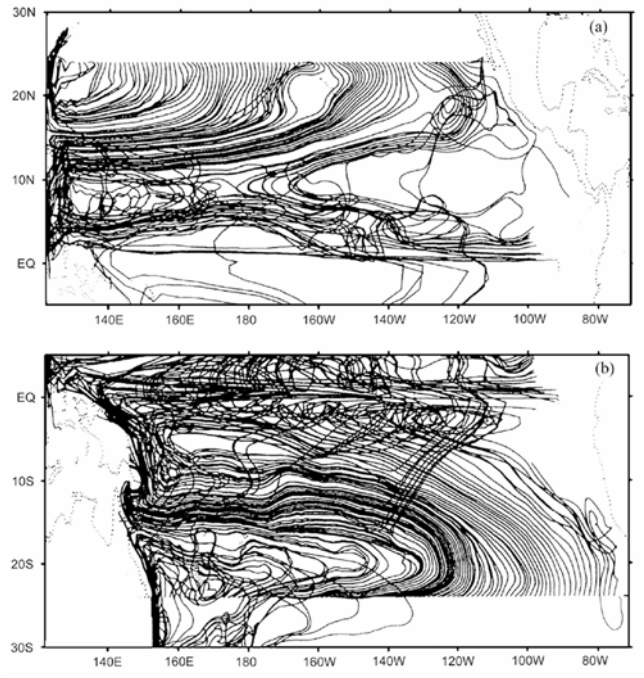

Figure 11. Trajectories of particles released in the Pacific (at the depth of 50 m) along (a) 24°N and (b) 24°S in the NCEP assimilated ocean model. The trajectories subducted in the central and eastern ocean basin penetrate into the equator in the low-latitude western boundary current and in the interior ocean, respectively, while the trajectories subducted in the western basin tend to recirculate poleward. Adapted from *Huang and Liu* [1999].

[42] The observational subtropical-tropical exchange is asymmetric about the equator. The North Pacific equatorward ventilation in the interior pathway is largely blocked by a potential vorticity ridge at about 10°N because of the wind stress associated with the Intertropical Convergence Zone [*Lu and McCreary*, 1995; *Liu and Huang*, 1998]; it is further weakened by the leaking through the Indonesian Throughflow into the Indian Ocean [*Rodgers et al.*, 1999]. The equatorward transports in the western boundary and interior pathways are estimated to be both 13 Sv in the South Pacific but 13 and 4 Sv, respectively, in the North Pacific. One climate implication of this asymmetric tropical-extratropical exchange is that the equatorial thermocline is controlled more by the South Pacific than the North Pacific (see section 4.2).

[43] The Atlantic STC is qualitatively similar to the Pacific. The smaller basin size, however, makes the interior pathway much weaker than the western boundary pathway [*Malanotte-Rizzoli et al.*, 2000; *Inui et al.*, 2002]. The equatorward transport is about 2 (4) Sv in the interior pathway [*Zhang et al.*, 2003] and about 3 (12) Sv in the western boundary pathway from the North (South) Atlantic. The much stronger equatorial asymmetry of the exchange in the Atlantic than in the Pacific is due to the strong return limb of the North Atlantic THC, which has a northward transport of about 16 Sv across the equator. The subtropical-tropical exchange in the Indian Ocean differs fundamentally from the Pacific and Atlantic. Subduction occurs predominantly in the south Indian Ocean because of the limited Indian Ocean north of the equator; the subsurface water upwells off equator because of the annual mean westerly wind and downwelling along the equator. The annual mean equatorial wind is dominated by a southeasterly wind turning to a southwesterly wind northward across the equator. The associated zonal wind stress forces a cross-equatorial cell, with a southward surface Ekman transport of 6 Sv and a northward thermocline return flow mainly along the western boundary in the Somali current, with part of the thermocline source waters contributed by the Indonesian Throughflow [*Schott et al.*, 2002]. The Indian Ocean STC is also characterized by a dramatic seasonal variability. The near-surface part of tropical Indian Ocean circulation reverses its direction with seasons because of the dramatic reversal of the surface monsoon winds.

3.2.3. Thermocline Adjustment and Wave Teleconnections

[44] Traditional studies on ocean ventilation focus on the mean flow and its transport of water properties. It is important, however, to point out that this transport of water property applies, in general, only to passive tracers. A temperature anomaly, in general, can be divided into two parts, the salinity-compensated part and the noncompensated part. The former is advected as a passive tracer because it induces no change of density, while the latter acts as an active tracer and propagates as a Rossby wave (section A2). Some oceanic thermocline temperature anomalies are indeed observed to follow the mean flow (Figure 4). This occurs because a subduction temperature anomaly in the thermocline tends to propagate as a long Rossby wave of higher baroclinic modes. Different from the first-mode long Rossby wave, which propagates westward regardless of the mean flow and which is generated predominantly by the wind forcing, these higher modes tend to be advected by the mean flow [*Liu*, 1999] (section A2), but at a speed slower than the mean flow [*Liu and Shin*, 1999; *Stephens et al.*, 2001], and tend to be forced by surface buoyancy forcing.

[45] Owing to the complex adjustment process the temporal evolution of the thermocline circulation may differ significantly from the time mean. In a recent OGCM study of the Pacific tropical-subtropical exchange, *Lee and Fukumori* [2003] and *Capotondi et al.* [2005] found that the interannual-decadal variability of the low-latitude western boundary transport is anticorrelated with that of the interior transport, opposite to the time mean, where both are in the same direction. Furthermore, the transport variability of the low-latitude western boundary current is much weaker than that of the interior transport in spite of a much larger time mean transport in the former. Preliminary analyses suggest that the compensation between the interior and western boundary transports is associated with the wind curl forcing, while the additional variability of the interior transport is associated with the zonal wind (surface Ekman flow) variability. A comprehensive theory of the temporal variability of the STC, however, is yet to be developed. In

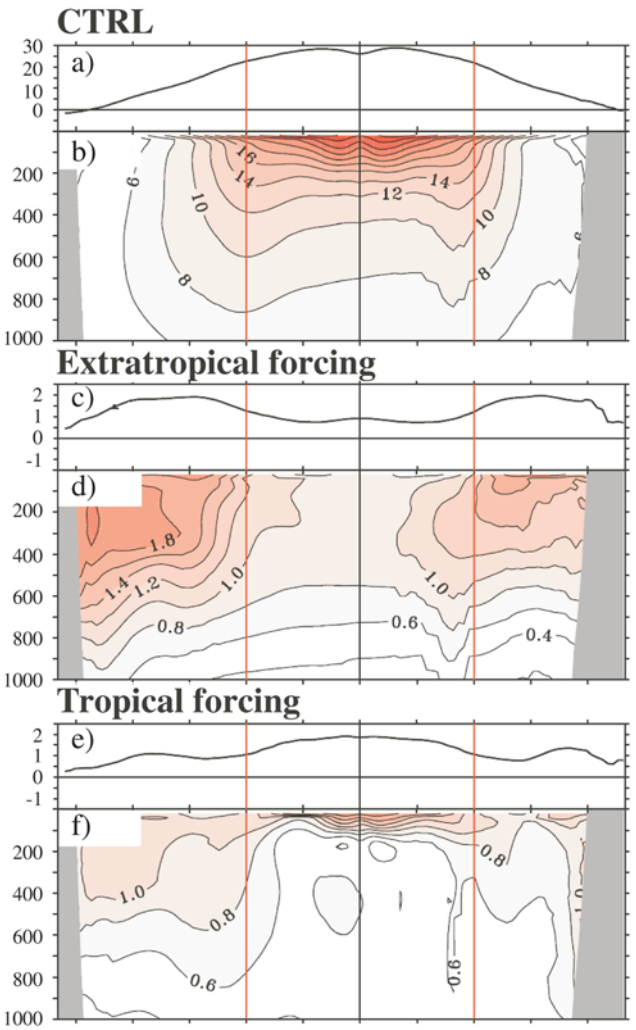

Figure 12. Responses of Pacific (a, c, and e) zonal mean SST and (b, d, and f) ocean temperature to a 2°C SST increase in a fully coupled ocean-atmosphere model. (top) Total SST (Figure 12a) and ocean temperature (Figure 12b) for the control simulation are shown, while the change of SST and temperature from the control are shown for the (middle) extratropical forcing run and (bottom) tropical forcing run. It shows that the remote response of extratropical SST to tropical forcing (Figure 12 bottom) is comparable with the remote response of tropical SST to extratropical forcing (Figure 12 middle). Adapted from *Liu and Yang* [2003].

principle, the STC is formed by the planetary Rossby waves across the basin as a part of thermocline adjustment process. The formation of the STC therefore takes years. Unlike the STC that is confined within and above the thermocline, the wind-induced Ekman transport, at very short timescales of weekly to monthly, is returned as a compensating barotropic flow from the surface to the bottom ocean and contributes to a strong seasonal variability of the oceanic heat transport [*Jayne and Marotzke*, 2001]. This heat transport variation, however, does not contribute significantly to the long-term surface ocean heat budget.

[46] As in the case of abyssal circulation adjustment (section 3.1.3) the western boundary coastal Kelvin wave also provides an alternative rapid teleconnection toward the equator [*Lysne et al.*, 1997; *Liu et al.*, 1999a; *Capotondi and Alexander*, 2001]. The Kelvin wave, combined with the long Rossby waves, can build weakly damped basin modes in a tropical-extratropical basin [*Cessi and Louazel*, 2001; *Liu*, 2002], which may be excited resonantly by the wind forcing to produce a response of preferred interdecadal timescales [*Cessi and Louazel*, 2001; *Liu*, 2003]. In the meantime the eastern boundary coastal Kelvin wave provides an oceanic teleconnection that transmits tropical climate variability, such as ENSO, into the extratropics (see section 4.1.2).

3.2.4. Teleconnections Beyond the Subtropics

[47] The equatorial subthermocline water can also be traced to higher latitudes from the subpolar regions. In the Pacific this water seems to originate mostly from the sub-Antarctic water near the Southern Ocean [*Toggweiler et al.*, 1991]. The penetration from the subpolar gyre into the subtropical gyre can be induced by the baroclinic exchange windows in the central western basin at the subtropical-subpolar gyre boundary [*Pedlosky*, 1984; *Schopp*, 1988; *Chen and Dewar*, 1993] and by the ventilation of the buoyancy-driven intermediate water [*Lu et al.*, 1998].

4. TELECONNECTIONS, CLIMATE VARIABILITY, AND CLIMATE CHANGE

[48] Much of the previous work on atmospheric and oceanic teleconnections has focused on the dynamics of the transport and wave processes in the atmosphere or ocean separately. However, the full climate impact of these teleconnections can only be assessed from the coupled perspective, because it involves feedbacks between the ocean and the atmosphere. In a recent coupled general circulation model (GCM) study [*Liu and Yang*, 2003] (Figure 12) the tropical impact on extratropical SST is assessed in a tropical forcing sensitivity experiment. In this experiment the ocean and atmosphere are decoupled within 30°, where the atmosphere is forced by a prescribed climatological SST plus a +2°C anomaly. This tropical warming is found to increase the remote extratropical SST by about 1°C (Figure 12 bottom), which is half of the tropical SST forcing anomaly and therefore represents a significant climate impact. Similarly, the extratropical impact on tropical climate is assessed in a complementary experiment with extratropical forcing. In this experiment the ocean and atmosphere are decoupled outside 30°, where the atmosphere is forced by a climatological SST plus a +2°C anomaly. The remote tropical SST is also increased by 1°C (Figure 12 middle). A comparison of the two sensitivity experiments suggests that the remote tropical impact of extratropical SST is as strong as the remote extratropical impact on tropical SST, a rather unexpected result since one tends to think that the tropics is more efficient in affecting the extratropics through the atmospheric teleconnection (see section 4.1). Further analyses and experiments indicate that while remote extra-

tropical warming by the tropical SST forcing (Figure 12 middle) is contributed entirely by the enhanced Hadley circulation, the remote tropical warming by extratropical SST forcing is accomplished by both the atmospheric (about 70%) and oceanic (about 30%) teleconnections; the Southern Hemisphere has a stronger remote climate impact than the Northern Hemisphere does [*Yang and Liu*, 2005]; the extratropical SST warming also weakens tropical variability of ENSO [*Yang et al.*, 2005]. This type of coupled ocean-atmosphere response between the heat transports of the Hadley cell and the STC has been suggested theoretically by *Held* [2001], although the quantitative aspects need to be confirmed by other models. Overall, this example demonstrates a significant remote climate impact due to the teleconnection. Recent studies further suggest that some fundamental features of climate change and climate variability depend critically on teleconnections. We first review the tropical impact on extratropical climate variability, mainly through the atmospheric teleconnection; we will then discuss extratropical influence on tropical climate through both the atmospheric and oceanic teleconnections; finally, we will study the role of interhemispheric THC climate teleconnections and global teleconnections.

4.1. Tropical Impact on Extratropical Climate Variability

4.1.1. Tropical Impact on Extratropical Climates

[49] The ENSO-driven large-scale atmospheric teleconnections (see section 2) alter the near-surface air temperature, humidity, and wind as well as the distribution of clouds far from the equatorial Pacific. The resulting variations in the surface heat, momentum, and freshwater fluxes can induce changes in SST, salinity, mixed layer depth (MLD), and ocean currents. Thus the atmosphere acts as a bridge between the equatorial Pacific and the global oceans [e.g., *Alexander*, 1990, 1992; *Luksch and von Storch*, 1992; *Lau and Nath* 1994, 1996; *Klein et al.*, 1999] (for an overview see *Alexander et al.* [2002]).

[50] During El Niño events, enhanced cyclonic circulation around the deepened Aleutian Low results in anomalous northwesterly winds that advect relatively cold dry air over the western North Pacific, anomalous southerly winds that advect warm moist air along the west coast of North America, and enhanced surface westerlies over the central North Pacific. The anomalous surface heat fluxes and the oceanic Ekman transport integrated over the MLD cool the ocean between 30°N and 50°N west of ~150°W and warm the ocean from the vicinity of Hawaii to the Bering Sea (Figure 13). In the central North Pacific the stronger wind stirring and negative buoyancy forcing increase the MLD, and the cold anomalies that extend through the mixed layer remain beneath the mixed layer when it shoals in spring. Some of this water is reentrained into the mixed layer in the following fall and winter via the "reemergence mechanism" [e.g., *Alexander et al.*, 1999, 2002], and some is subducted entering the thermocline and flowing equatorward [*Schneider et al.*, 1999].

[51] Studies using AGCM–mixed layer ocean model simulations have confirmed the basic bridge hypothesis for forcing North Pacific SST anomalies but have reached a different conclusion on the impact of these anomalies on the atmosphere [*Alexander*, 1992; *Bladé*, 1999; *Lau and Nath*, 1996, 2001]. Recent model experiments suggest that the oceanic feedback on the extratropical response to ENSO is complex but of modest amplitude; that is, atmosphere-ocean coupling outside of the tropical Pacific slightly modifies the atmospheric circulation anomalies in the PNA region, but these modifications depend on the seasonal cycle and air-sea interactions both within and beyond the North Pacific Ocean [*Alexander et al.*, 2002].

[52] Most studies of the atmospheric bridge have focused on boreal winter since ENSO, and the associated atmospheric circulation anomalies peak at this time. However, significant bridge-related changes in the climate system also occur in other seasons. Over the western North Pacific the southward displacement of the jet stream and storm track in the summer prior to when ENSO peaks changes the solar radiation and latent heat flux at the surface, which results in anomalous cooling and deepening of the oceanic mixed layer at ~40°N [*Alexander et al.*, 2004b; *Park and Leovy*, 2004]. The strong surface flux forcing in conjunction with the relatively thin mixed layer in summer leads to the rapid formation of large-amplitude SST anomalies in the Kuroshio extension region. These SST anomalies may influence large-scale climate variability including the location of marine stratus cloud decks [e.g., *Norris and Leovy*, 1994; *Klein et al.*, 1995; *Norris*, 2000] and summer rainfall over Asia and North America [*Ting and Wang*, 1997; *Lau and Weng*, 2002].

4.1.2. ENSO's Impact on PDV

[53] *Zhang et al.* [1997] utilized several analysis techniques to separate interannual ENSO variability from a residual containing the remaining (>7 years) "interdecadal" variability. The pattern based on low-pass-filtered data is similar to the unfiltered ENSO pattern, except it is broader in scale in the eastern equatorial Pacific and has enhanced magnitude in the North Pacific relative to the tropics (Figure 14). The low-frequency ENSO pattern is also similar to the leading pattern of monthly North Pacific SST, which exhibits pronounced low-frequency fluctuations and was thus termed the Pacific Decadal Oscillation (PDO) by *Mantua et al.* [1997]. The atmospheric bridge from the tropical Pacific can impact the PDV either through variability in the surface forcing at decadal timescales [*Trenberth*, 1990; *Graham et al.*, 1994; *Deser et al.*, 2004b] or by ENSO-related forcing on interannual timescales, which is subsequently integrated, or "reddened," by ocean processes including the reemergence mechanism [*Newman et al.*, 2003; *Schneider and Cornuelle*, 2005]. Model experiments and data reconstruction techniques suggest that ~1/3 of PDO variability on timescales >10 years is due to forcing from the central and eastern tropical Pacific, although uncertainties in estimating low-frequency SST variability and forcing from other portions of the tropical Pacific and Indian Oceans could enhance the fraction of North Pacific

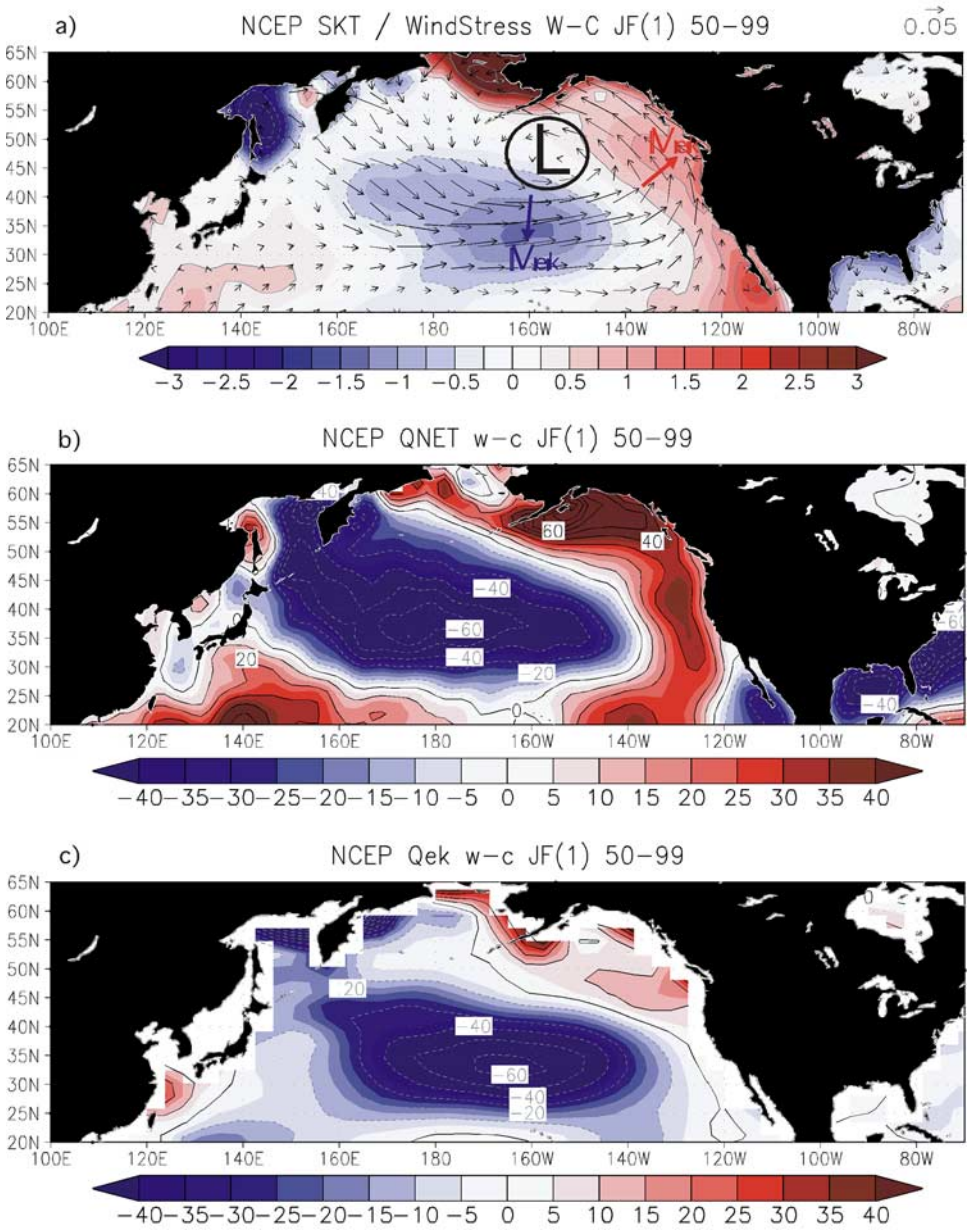

Figure 13. El Niño–La Niña composite average of (a) surface wind stress vectors (N m^{-2}, scale vector in upper right) and SST (shading interval 0.25°C), (b) net surface heat flux, and (c) Ekman transport in flux form during January and February as obtained from NCEP reanalysis for ENSO events during the period 1950–1999. Figures 13a–13c depict the influence of the atmospheric bridge associated with ENSO on the North Pacific Ocean. In Figure 13a the L represents the center of the anomalous negative sea level pressure anomaly associated with a deeper Aleutian Low, and the red (blue) arrow indicates the direction of Ekman transport that warms (cools) the ocean. The shading (contour) interval is 5 (10) W m^{-2} in Figures 13b and 13c; positive (negative) values indicate fluxes that warm (cool) the ocean.

SST variability due to teleconnections from the tropics [*Newman et al.*, 2003; *Deser et al.*, 2004b]. The PDO is only a partial measure of PDV, and some of the decadal variability in the North Pacific, particularly variability in the Kuroshio extension, is independent of forcing from the tropics [e.g., *Nakamura et al.*, 1997; *Barlow et al.*, 2001].

[54] ENSO can also generate extratropical Pacific oceanic variability through the oceanic teleconnection of the coastal Kelvin wave. The equatorial thermocline variability associated with ENSO excites coastal Kelvin waves, which propagate poleward along the eastern boundary in both hemispheres, generating substantial coastal sea level variability [*Enfield and Allen*, 1980; *Chelton and Davis*, 1982; *Clarke and Levedev*, 1997]. In the meantime the coastal Kelvin wave also generates long Rossby waves propagating westward across the extratropical Pacific, generating substantial interannual oceanic variability in the entire Pacific

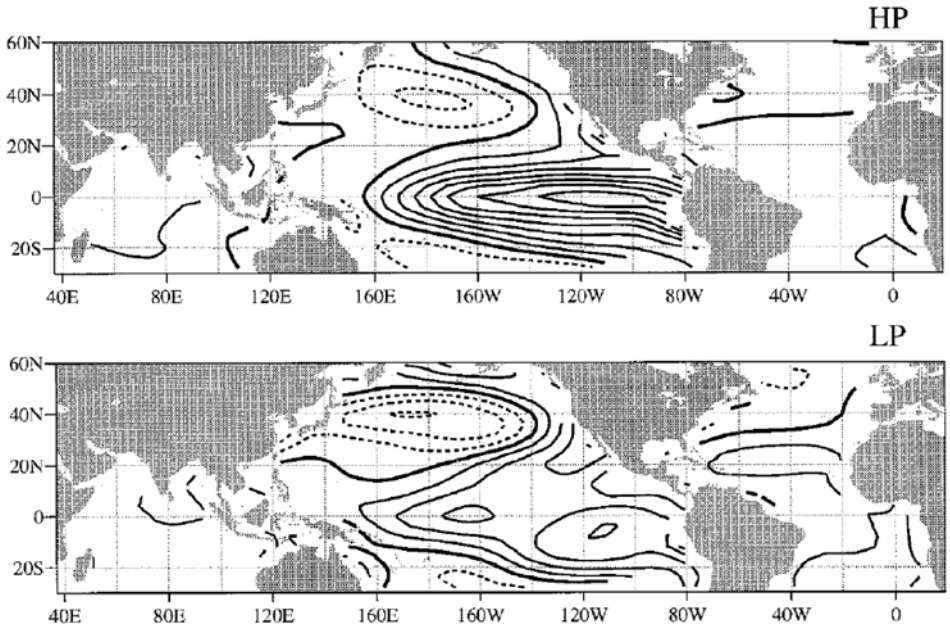

Figure 14. SST patterns regressed with the leading (normalized) principal components of 6-year high-pass (HP) and low-pass (LP) filtered SST over the Pacific domain. Negative contours are dashed, and the zero contour is bold. The high-pass pattern represents the interannual ENSO variability, while the low-pass pattern represents the Pacific decadal variability. The Pacific decadal variability shows substantial SST variability in both the tropical and North Pacific, which prompted the speculation that Pacific Decadal Oscillation may be related to extratropical-tropical interactions. Adapted from *Zhang et al.* [1997]. Reprinted with permission courtesy of the American Meteorological Society.

[*Jacobs et al.*, 1994; *Chelton and Schlax*, 1996; *Miller et al.*, 1997].

4.1.3. Teleconnections From the Tropical Atlantic to the North Atlantic

[55] Observations indicate that tropical Atlantic SST anomalies in summer and fall are linked with the NAO in the following winter [e.g., *Czaja and Frankignoul*, 2002]. SST forcing in the tropical Atlantic induces a strong wave-like response in AGCM experiments during October and November. Coupling the AGCM with a slab ocean in the North Atlantic improves the representation of the midlatitude response relative to uncoupled simulations, as the interaction between the midlatitude SST, low-frequency circulation, and extratropical storm track activity reinforces and maintains the NAO until winter [*Drevillon et al.*, 2003; *Peng et al.*, 2005]. However, the teleconnection from the tropics is overwhelmed by the local internal atmospheric variability over the North Atlantic.

4.2. Extratropical Impact on Tropical Climate Variability

4.2.1. Extratropical-Tropical Interaction and PDV

[56] The attempt to understand PDV [*Zhang et al.*, 1997; *Mantua et al.*, 1997] has stimulated great interest in the role of extratropical-tropical interaction in climate, especially its role in decadal memory. At decadal timescales the midlatitude ocean is usually thought to play a more important role because of its natural memory associated with slow Rossby waves (section A2) and ocean currents. This led *Latif and Barnett* [1994] to hypothesize that PDV is induced by thermocline memory and positive ocean-atmosphere feedback within the extratropical North Pacific. Further studies indicate that PDV exhibits a strong SST signature not only in the North Pacific but also in the tropical and South Pacific (Figure 14) [*Garreaud and Battisti*, 1999; *Evans et al.*, 2001; *Deser et al.*, 2004b]. In the meantime, preliminary analyses of North Pacific temperature variability show signs of a ventilation of a decadal temperature anomaly toward the lower latitudes [*Deser et al.*, 1996] (Figure 4). These led *Gu and Philander* [1997] to hypothesize that PDV depends on tropical-extratropical interactions. In their original hypothesis an initial warm SST anomaly on the equator is first amplified by the Bjerknes wind-upwelling positive feedback: The warm anomaly weakens the equatorial trade wind and, in turn, equatorial upwelling, which further amplifies the initial warming. Meanwhile, the atmospheric response to warm tropical SST intensifies the midlatitude westerly wind in the central North Pacific. The increased surface westerlies cool the midlatitude SST through an increased latent heat loss and southward cold Ekman advection (see section 4.1). The cold surface water is then ventilated into the equatorial thermocline in about a decade (see section 3.2), providing a delayed negative feedback that suppresses the initial warming and eventually switches the sign of the equatorial SST. This completes half the cycle of the decadal variability. Here the PDV derives its memory from the extratropical ocean through oceanic teleconnection, while it gains its strength through positive

ocean-atmosphere feedback and atmospheric teleconnection, showing the crucial roles of both the atmospheric and oceanic teleconnections.

[57] In spite of its instrumental role in stimulating the studies on tropical-extratropical interaction the original Gu-Philander hypothesis is now recognized as being deficient for explaining the observed Pacific decadal variability. The role of oceanic ventilation is questioned by a careful model-observation study [*Schneider et al.*, 1999], which shows that the observed North Pacific temperature anomaly fails to reach the equator. Nevertheless, there is some evidence that the equatorial Pacific may be affected by the ventilation from the subtropical South Pacific [*Wang and Liu*, 2000; *Luo and Yamagata*, 2001], consistent with the equatorial asymmetry of the Pacific tropical-extratropical exchange (see section 3.2). Therefore the Gu-Philander hypothesis may still remain viable if the ventilation originates from the South Pacific rather than the North Pacific. An alternative hypothesis has been proposed by *Kleeman et al.* [1999] (see also *Solomon et al.* [2003]), based on the study of a coupled model of intermediate complexity. They suggest that the equatorial thermocline is cooled by an enhanced STC transport of the cold extratropical water (as opposed to the mean current transport of a cold temperature anomaly in the Gu-Philander hypothesis). This proposal seems to be consistent with recent observations that the STC transport exhibits noticeable interdecadal changes associated with the PDV [*McPhaden and Zhang*, 2002]. Another alternative is proposed by *Schneider* [2000] based on the analysis of an OGCM simulation. In this so-called ''spiceness mode'' the equatorial temperature is affected by the equatorward ventilation of salinity-compensated temperature anomalies.

[58] It is generally difficult to identify the role of teleconnection on PDV in the coupled climate based on the observation, or a control simulation, alone. This is because the observed PDV is already the final product after complex ocean-atmosphere feedbacks. With a coupled model, however, sensitivity experiments can be performed to determine the role of teleconnection explicitly. *Liu et al.* [2002] and *Wu et al.* [2003] performed sensitivity experiments using various modeling surgery strategies such that ocean-atmosphere interaction and oceanic teleconnection can be turned on and off in different regions. These experiments demonstrate, unambiguously in the context of their model, that the tropical Pacific and North Pacific each have its own decadal mode, called the Tropical Pacific Mode and North Pacific Mode, respectively. The origins of these modes are independent of tropical-extratropical interaction. Nevertheless, both modes can be enhanced significantly by tropical-extratropical teleconnections. For example, tropical Pacific decadal SST variance is almost doubled with the presence of extratropical ocean-atmosphere interaction and the oceanic teleconnection. This implies that PDV consists of multiple decadal variability modes, which can interact with each other through tropical-extratropical interactions. Further studies, however, are still needed to understand the mechanism for each decadal variability mode and how teleconnections affect each mode. It also remains unclear how the temporal variability of the STC [*Lee and Fukumori*, 2003] is related to the decadal variability of these coupled modes.

4.2.2. Impact of Oceanic Teleconnection

[59] The impact of equatorward ventilation on tropical climate tends to increase with both the temporal and spatial scales of the variability. Equatorward ventilation seems to be critical for basin-scale climate changes at centennial and longer timescales, such as the maintenance of the climatological equatorial thermocline and its long-term response to global warming [*Shin and Liu*, 2000; *Liu and Yang*, 2003] and past climate forcings [*Liu et al.*, 2002, 2003]. At interdecadal or shorter timescales, ventilation appears less effective than the first-mode baroclinic Rossby wave. In addition, the North Pacific winter SST anomaly associated with the PDV exhibits subbasin-scale features, with opposite signs between the Kuroshio extension region and the surrounding region. These surface anomalies of the opposite signs may cancel each other during ventilation because of along-isopycnal mixing, further damping the ventilation signal toward the equator [*Nonaka and Xie*, 2000].

[60] The coastal Kelvin wave also provides an important equatorward oceanic teleconnection along the western boundary (section 3.2). Besides its importance to the adjustment of the abyssal circulation [*Kawase*, 1987] and overturning circulation [*Johnson and Marshall*, 2002], recent studies further suggest that the coastal Kelvin wave may help extratropical decadal variability to impact the tropical upper oceans in the Pacific [*Lysne et al.*, 1997] and Atlantic [*Yang*, 1999]. This teleconnection to the tropical SST can further impact global tropical climate through atmospheric teleconnections of equatorial Kelvin wave and Walker circulation [*Dong and Sutton*, 2002; *Zhang and Delworth*, 2005].

4.2.3. Impact of Atmospheric Teleconnection

[61] While the atmospheric bridge primarily extends from the tropics to the extratropics, variability originating in the North Pacific may also influence the tropical Pacific. On the global scale the change of midlatitude climate can change the storm track activity, the associated eddy heat and momentum fluxes, and the Hadley circulation (as shown in the example of Figure 12 middle). On regional to basin scales, *Barnett et al.* [1999] and *Pierce et al.* [2000] proposed that the atmospheric response to slowly varying SST anomalies in the Kuroshio extension region extends into the tropics, thereby affecting the trade winds and decadal variability in the ENSO region. *Vimont et al.* [2001, 2003] found that tropical variability can be generated by the extratropical atmosphere via the ''seasonal footprinting mechanism.'' Large fluctuations in internal atmospheric modes over the North Pacific in winter impart an SST ''footprint'' onto the ocean via changes in the surface heat fluxes. The SST footprint, which persists through summer in the subtropics, impacts the atmospheric circulation including zonal wind stress anomalies that extend onto and south of the equator. These zonal wind stress anomalies are an important element of the stochastic forcing of interannual and decadal ENSO variability [*Vimont et al.*, 2003]. A

similar midlatitude influence on the tropics is found in the Atlantic [*Czaja et al.*, 2002; *Chiang and Vimont*, 2004].

[62] Changes in sea ice can impact air-sea interaction over the adjacent ocean basins [e.g., *Deser et al.*, 2000] and have the potential to affect the tropics through the atmospheric teleconnection as well. *Chiang and Bitz* [2005] found a strong influence of ice on the marine Intertropical Convergence Zone (ITCZ) in an AGCM coupled to a 50-slab ocean. The ice induces cooling and drying of the air over the entire polar region, which is subsequently advected equatorward, resulting in cooler SSTs. When the relatively cold SSTs extend into the tropics of that hemisphere, the ITCZ is displaced toward the opposite hemisphere. This mechanism may be applicable to past climates like the Last Glacial Maximum, when asymmetric changes in ice cover between hemispheres occurred [*Chiang et al.*, 2003].

4.2.4. Coupled Ocean-Atmosphere Teleconnection

[63] Equatorward teleconnection can also be generated by ocean-atmosphere coupling. In an attempt to explain the origin of the equatorial annual cycle in the Pacific and Atlantic, *Liu and Xie* [1994] proposed a rapid coupled teleconnection that transmits subtropical climate signals into the equator in months. A warm SST anomaly north of the equator induces a low pressure and cyclonic flow, with a westerly anomaly to the south. This westerly anomaly weakens the climatological easterly and the associated latent heat loss, resulting in an equatorward propagation of the warm anomaly. Different from the teleconnections discussed previously in the atmosphere or ocean alone, the existence of this teleconnection depends on the coupling between the atmosphere and ocean. This equatorward coupled teleconnection was later used to understand the equatorward propagation of North Pacific decadal variability [*Wu et al.*, 2001, 2005] and the influence of NAO on tropical Atlantic variability [*Xie and Tanimoto*, 1998]. The seasonal footprint mechanism of *Vimont et al.* [2001, 2003] can also be regarded as a type of coupled teleconnection, because it depends on the processes in both the atmosphere and ocean. Recently, it has been proposed that this fast coupled equatorward teleconnection can work in phase with the slow STC oceanic teleconnection effectively as a relay teleconnection that allows the North Pacific decadal climate variability to generate decadal variability in the tropics [*Wu et al.*, 2007].

4.3. Interhemispheric and Global Climate Interactions

[64] Climate variabilities in the two hemispheres can impact each other through atmospheric and oceanic teleconnections. At long timescales the atmosphere continuously mixes climate signals across the equator, while the THC provides an effective oceanic channel for interhemisphere interaction (see section 3.1). In contrast to the atmospheric bridge the oceanic tunnel can retain the structure of anomalies over hundreds, and even thousands, of years. Paleoclimate proxies suggest that the THC was substantially shallower and perhaps weaker in the North Atlantic during the LGM than at present [e.g., *Duplessy et al.*, 1988]. A similar retreat of NADW is also implied in benthic foraminifera $\delta^{13}C$ for millennia cold climate events such as the Young Dryas [e.g., *Boyle and Keigwin*, 1987] and during early glacial times [*Keigwin et al.*, 1994]. The cause of the THC change, however, has remained controversial. Recent observational and modeling studies indicate that the change in the THC and associated climate indices over the North Atlantic may depend on interhemispheric teleconnections.

4.3.1. North Atlantic View and "Bipolar Seesaw"

[65] Many studies on fluctuations in the THC tend to emphasize the role of the North Atlantic freshwater forcing [e.g., *Broecker and Denton*, 1989; *Stocker*, 2000; *Alley et al.*, 2002]. One leading hypothesis is the "bipolar seesaw" [*Broecker*, 1998], where the injection of melting water over the North Atlantic weakens the THC, and the accompanying northward heat transport from the South Atlantic into the North Atlantic, leading to a surface cooling over the North Atlantic but warming over the South Atlantic (Figure 15a). Furthermore, the induced SST changes can affect global climate through global teleconnections in the atmosphere [*Dong and Sutton*, 2002; *Zhang and Delworth*, 2005] and ocean [*Huang et al.*, 2000; *Cessi et al.*, 2004; *Johnson and Marshall*, 2004]. These studies imply a North Atlantic lead to the southern climate change.

4.3.2. Southern Ocean View and Pole-Pole Circulation

[66] The Southern Ocean is also able to influence the THC in the North Atlantic through interhemispheric teleconnections. This impact can be forced by an anomalous surface wind stress [*Toggweiler and Samuels*, 1995], moisture transport/freshwater forcing [*Wang et al.*, 1999; *Weaver et al.*, 2002], and heating or cooling [*Knorr and Lohmann*, 2003]. Especially important is the freshwater forcing over the Southern Ocean, which, in the pole-pole THC model, determines the final equilibrium response of the world ocean THC [*Rooth*, 1982]. The critical role of the Southern Ocean salinity forcing is supported by recent simulations of glacial climate in a fully coupled GCM [*Shin et al.*, 2003]. From the coupled ocean-atmosphere–sea ice perspective these experiments suggest that the strong sea ice albedo sensitivity to long-term climate change over the Southern Ocean plays a dominant role in driving the North Atlantic THC. The strong basal heat flux associated with mixing in the deep ocean limits the sea ice thickness to about 1 m in the Southern Ocean. Given the dependence of the positive sea ice albedo feedback on the ice area, widespread changes in the thin sea ice cover over the Southern Ocean make it more sensitive to climate forcing than the Arctic, which is covered by thick sea ice. Therefore long-term global cooling greatly enhances the sea ice extent, and thus the brine injection, over the Southern Ocean, which increases the density and, in turn, the northward penetration of the AABW, leading to a shallower and weaker THC in the North Atlantic (Figure 16). This Southern Ocean impact on the THC occurs despite the nearly uniform global radiative forcing associated with reduced concentrations of atmospheric CO_2. Indeed, similar results are obtained in simu-

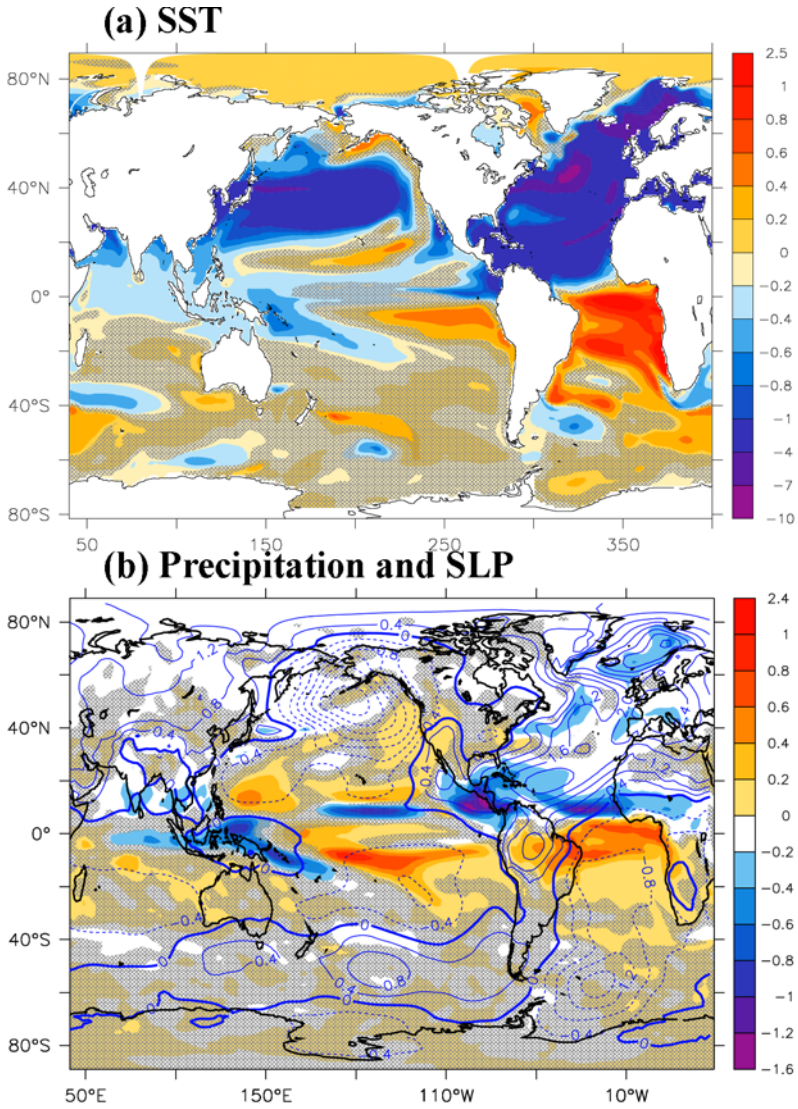

Figure 15. Response of global (a) SST and (b) precipitation and sea level pressure (SLP) to a freshwater forcing over the northern North Atlantic in a fully coupled ocean-atmosphere GCM. The experiment is integrated for 60 years after a freshwater flux of 0.6 Sv is imposed. The maximum Atlantic THC rapidly weakens from 16 Sv to about 6 Sv after about 20 years. The northward heat transport in the global ocean is reduced by 0.28 PW but increased by 0.32 PW. The North Atlantic SST shows a bipolar seesaw pattern. The SST anomaly also forces the atmosphere, which then teleconnects throughout the tropics rapidly. Adapted from *Zhang and Delworth* [2005]. Reprinted with permission courtesy of the American Meteorological Society.

lations in which only the atmospheric CO_2 concentrations are reduced [*Liu et al.*, 2005].

4.3.3. A Unified View With Different Timescales

[67] The apparent contradiction between the northern and southern lead views may be reconciled if one considers the timescales of the dominant processes in the two basins. The Southern Ocean driving mechanism is efficient only at timescales longer than millennia because of the slow (millennial) adjustment of the Southern Ocean temperature and salinity. This slow response time might be lengthened further by the response time of the carbon cycle, which is mainly associated with the Southern Ocean during glacial cycles and may play a critical role for glacial cycles [*Sarmiento and Toggweiler*, 1984; *Shackleton*, 2000; *Archer et al.*, 2000]. At timescales shorter than 1 millennia, the North Atlantic driving may dominate because of the rapid adjustment time of THC in the North Atlantic (see section 3.1). The effect of the different THC response to transient and equilibrium moisture transport forcing has been shown in a hybrid coupled ocean-atmosphere model [*Wang et al.*, 1999]. Consistent with *Rooth*'s [1982] THC model, the equilibrium response of the THC in the North Atlantic weakens with an increased salinity forcing of the Southern Ocean. Nevertheless, during initial transient adjustment the THC is primarily affected by the forcing over the North Atlantic. The difference between the transient and equilibrium response has been used to interpret the similar thermohaline collapse in both the global warming experi-

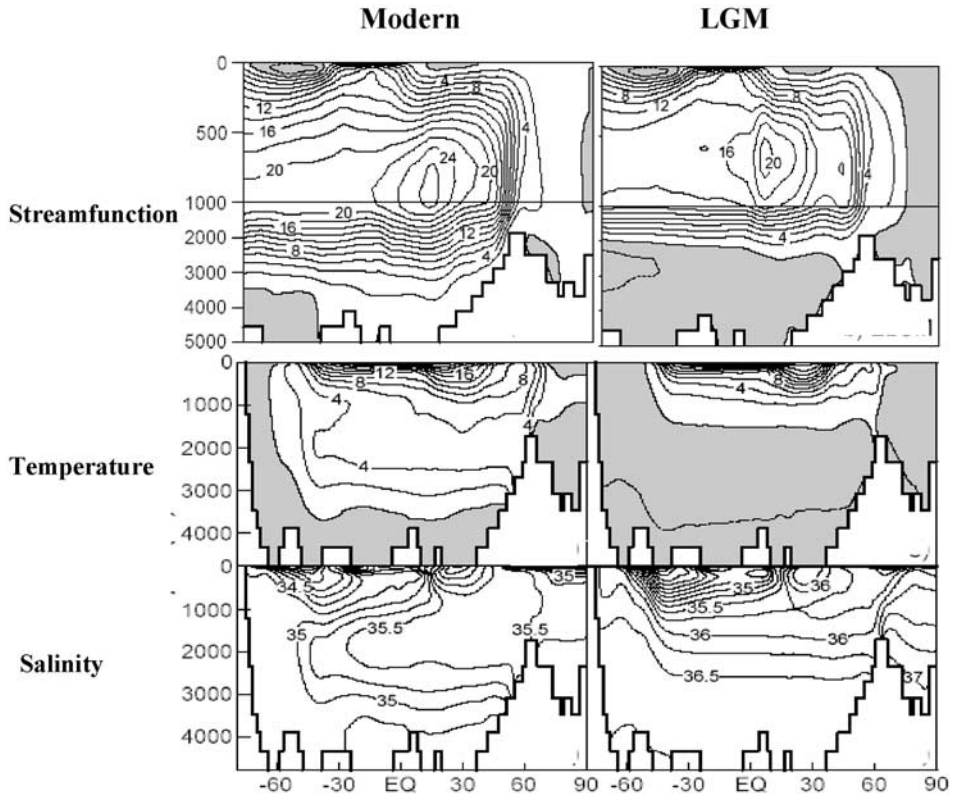

Figure 16. Total overturning stream function (shading indicating negative values), zonal mean temperature (°C) (shading indicating negative values), and salinity (ppt) in the Atlantic as simulated in the NCAR-Climate System Model version 1.0 for the modern and Last Glacial Maximum. Compared with the modern, at LGM the THC is shallower by 1000 m as implied by the proxy records; the temperature and salinity below 2 km is virtually uniform, dominated by the enhanced AABW. These features are consistent with recent observations [*Adkins et al.*, 2002]. Further diagnosis shows that the enhanced AABW is caused by an enhanced brine injection in the Southern Ocean and interhemispheric teleconnection. Adapted from *Liu et al.* [2005].

ments and global cooling glacial climate [*Marotzke*, 2000]. A coupled GCM study of THC change due to increased CO_2 forcing [*Manabe and Stouffer*, 1994] indicated that the THC first weakens in the initial hundreds of years in response to the increased moisture transport to the North Atlantic but later recovers after thousands of years. This disparity between the response times of the two hemispheres can be seen clearly in a recent fully coupled GCM study [*Stouffer*, 2004]. With a largely uniform CO_2-induced climate forcing the hemispheric surface air temperature equilibrates in hundreds of years in the Northern Hemisphere but in thousands of years in the Southern Hemisphere. Hence the difference in the response times may lead to a unified view of the past THC change [*Liu et al.*, 2005]: The North Atlantic forcing is dominant for millennial THC variability, while the Southern Ocean, together with the associated positive climate-CO_2 feedback [e.g., *Francois et al.*, 1998; *Stephens and Keeling*, 2002], becomes the dominant forcing for glacial/interglacial THC changes. This unified view is largely consistent with the available paleoclimate evidence [*Liu*, 2006]. For example, the lagged correlation of the ice core $\delta^{18}O$ between the Antarctic and Greenland [*Steig and Alley*, 2003; *Wunsch*, 2003] shows a clear lead of 1–2 kyr of the Antarctic at glacial-interglacial timescales but no clear lead-lag relation toward the millennial timescales for Heinrich and Dansgaard/Oeschger events. Composite millennial events in the ice cores [*Schmittner et al.*, 2003] and SST reconstruction [*Lynch-Steiglitz*, 2004] also suggest an antiphase "seesaw" response.

4.3.4. The Tropics and Its Role in Global Teleconnections

[68] The tropical Pacific Ocean may significantly influence North Atlantic and global climate variability from millennial to orbital timescales [*Cane*, 1998; *Clement et al.*, 1999], providing another challenge to the traditional view of North Atlantic control over low-frequency climate fluctuations. Analogous to the present climate variability, long-term changes of tropical Pacific SST can impact the North Atlantic through the PNA atmospheric teleconnection (see section 2.2). For example, a cold tropical Pacific cools the northern part of North America and the North Atlantic [*Yin and Battisti*, 2001] and therefore may trigger high-latitude glaciation. The tropical Pacific, however, does not have a long memory, so it is unclear how it can be the sole driver of global climate except for ENSO variability.

[69] The tropical Pacific may impact climate at low frequencies if it varies in conjunction with other ocean basins. In glacial climate evolution, for example, the Southern Ocean can first affect the tropics through both atmospheric and oceanic teleconnections, and then the tropical SST impact global climate through atmospheric teleconnections. Southern Hemisphere control of tropical Pacific SST is supported by coupled model simulations of past [*Liu et al.*, 2002] and present [*Yang and Liu*, 2005] climates. It also appears to be consistent with paleoclimate evidence of glacial cycles, which show an evolution of atmospheric CO_2 in phase with the air temperatures in the Antarctic and tropics but leading the Greenland air temperature and continental ice volume by a few thousand years [*Shackleton*, 2000; *Visser et al.*, 2003]. Similarly, for millennial timescales the North Atlantic climate variability may affect the tropical Atlantic through atmospheric and oceanic teleconnections, including the bipolar seesaw (Figure 15a); the tropical Atlantic then further impacts the global tropical atmosphere through atmospheric Kelvin waves and the Walker circulation (Figure 15b) [*Dong and Sutton*, 2002; *Zhang and Delworth*, 2005]. This global teleconnection seems to be consistent with paleoclimate records, which suggest that tropical monsoon climate follows the millennial climate variability from the North Atlantic [*Wang et al.*, 2001; *Yuan et al.*, 2004]. Although the magnitude remains uncertain, the North Atlantic may also impact tropical Indian and Pacific oceans through the teleconnection of the oceanic Rossby wave and Kelvin wave at centennial timescales (see sections 3.1.3 and 3.2.3). The tropical Indian and Pacific oceans can then impact global climate through the atmospheric teleconnection (see section 2.2). Therefore, in these scenarios, the tropics act as a relay, transmitting high-latitude signals to the entire globe via atmospheric teleconnections.

5. CONCLUSIONS AND DISCUSSIONS

[70] Recent advances in our understanding of atmosphere and ocean teleconnections are reviewed, with an emphasis on how atmospheric bridges and oceanic tunnels impact variability in the coupled climate system. Atmospheric teleconnections provide an effective means for tropical SSTs to influence extratropical climate variability. Surface temperature anomalies in the tropics influence the upper atmosphere through deep convection. The associated diabatic heating anomalies impact the subtropical and extratropical atmosphere through the Hadley cell, stationary waves, and interactions with midlatitude storm tracks. By comparison, the atmospheric response to surface ice and temperature anomalies in middle and high latitudes appears to be smaller and less robust. However, extratropical surface conditions appear to impact the frequency of occurrence of some teleconnection patterns. Internal atmospheric processes, such as interactions between midlatitude storms and the jet stream, also generate teleconnection patterns. Both the internal and surface-forced extratropical atmospheric anomalies can extend into the tropics and have some influence on ENSO and decadal climate variability, although this equatorward atmospheric bridge may be in the form of random forcing rather than a deterministic process with a set timescale.

[71] Beyond the classical gyre circulation the dynamics of oceanic teleconnection have advanced in several areas and appears to be important in transmitting extratropical climate signals to the tropics or to the other hemisphere. First, the shallow STC is recognized as an important ocean tunnel connecting the tropical and extratropical oceans. The STC is driven by the surface Ekman flow, with the exchange transport determined by the wind stress on the tropical-subtropical boundary. Over both the Pacific and Atlantic the STC exchange is stronger in the Southern Hemisphere, implying a stronger southern control on the equatorial ocean. Temporal variability of the STC, however, remains poorly understood. Second, the pole-pole interhemispheric THC model is recognized as a better analogue for the observed THC than the equator-pole paradigm. Relative to thermocline dynamics, however, the THC remains poorly understood from both an observational and theoretical viewpoint, which is further undercut by our limited knowledge of the diapycnal mixing in the ocean, adding greater uncertainty to the role of THC in climate change. Third, recent studies have led to a largely unified framework for both the steady circulation and wave propagation, in which ocean waves provide an effective means for basin- to global-scale teleconnections at decadal to centennial timescales.

[72] One important difference between the teleconnections in the atmosphere and ocean lies in their dramatically different timescales. Almost all atmospheric teleconnections are fast, usually reaching equilibrium in less than a season. In contrast, oceanic teleconnections span a wide range of timescales from interannual to decadal to centennial and even over millennia. In principle, a teleconnection mechanism becomes fully effective only for climate variability of comparable or longer timescales. Therefore the atmospheric teleconnections should, in principle, be effective for all the climate variability on interannual and longer timescales. Oceanic teleconnections, on the other hand, will be fully effective only for climate variability at periods longer than their adjustment timescale. Thus oceanic teleconnection provides long-term memory that is critical for many types of climate variability, while the atmosphere provides stochastic forcing that can help excite the low-frequency ocean fluctuations.

[73] Most uncertain yet is the role of teleconnections in climate change and climate variability in the coupled ocean-atmosphere system. Except for ENSO's impact the climatic effects of other teleconnections remain speculative, and, in most cases, they are not well quantified. For example, the role of tropical-extratropical interaction in PDV remains inconclusive; the role of interhemispheric interaction in the change of THC also remains speculative at this stage. Therefore a future challenge is to understand and assess the full impact of teleconnections in the ocean-atmosphere-ice system.

[74] Finally, we discuss the role of teleconnections in the global mean climate, which has so far received limited attention in the literature. Paleoclimate records indicate that previous climate change events included adjustments in the meridional temperature distribution in addition to changes in the global mean temperature. Climate change is often characterized by small anomalies in the tropics and large anomalies at high latitudes, which may induce large changes in the poleward energy transport. The change of global mean could be a by-product of changes in the equator-pole gradient and, in turn, the meridional energy transport [*Lindzen*, 1994].

[75] Part of the global rectification effect due to teleconnection can be discussed in a pedagogic climate model. The global atmosphere is divided into the tropical (column 1) and extratropical (column 2) columns of equal surface area. The heat budget for the two columns is

$$0 = -\lambda_1 T_1 - Q + S_1, \qquad 0 = -\lambda_2 T_2 + Q + S_2,$$

where $S_{1,2}$, $T_{1,2}$, and $\lambda_{1,2}$ represent the effective climate forcing, temperature, and damping, respectively; $Q > 0$ is the poleward heat transport and could depend on the temperature contrast. Without teleconnection $Q = 0$, temperatures are simply the local radiative equilibrium temperatures $T_{1,2E} = S_{1,2}/\lambda_{1,2}$, and the global mean is also its radiative equilibrium temperature $T_{GE} = T_{1E} + T_{2E}$. With the heat transport the temperature contrast is reduced as expected. Moreover, the global mean temperature $T_G = T_1 + T_2$ is also changed such that it differs from the radiative equilibrium temperature as

$$T_G - T_{GE} = (\lambda_1 - \lambda_2)Q/\lambda_1\lambda_2.$$

Therefore the global mean temperature differs from the radiative equilibrium temperature as long as the climate sensitivity is spatially inhomogeneous. Since climate sensitivity differs substantially among regions [*Boer and Yu*, 2003a, 2003b], it is conceivable that teleconnections can indeed impact global mean climate. Furthermore, global temperature will be higher (lower) than its equilibrium temperature if the damping is stronger (weaker) in the tropics than in the extratropics. Then, the teleconnection acts as an amplifier (regulator) for global mean temperature. Physically, when some heat is transported from the tropics to the extratropics, the warming in the extratropics more (less) than offsets the cooling in the tropics, because the extratropical climate response is less (more) damped. It is likely that the tropics have a stronger damping than higher latitudes. This is because the tropics have a higher temperature and, in turn, latent heating and long-wave radiation damping, while the high latitude has the positive snow-ice- albedo feedback, which tends to reduce the damping there. Therefore teleconnection may act as an amplifier to global mean climate. This has been shown recently in another conceptual two-column model [*Cai*, 2005]. The same idea can be applied to the combined tropical-subtropical region as the "globe" domain and the tropics and subtropics as the two subregions [*Pierrehummbert*, 1995; *Seager and Murtugudde*, 1997; *Miller*, 1997; *Clement and Seager*, 1999]. Now, the "global" rectification effect leads to a negative feedback and, in turn, a thermostat regulator for the combined tropical-subtropical climate, because of a higher damping rate in the subtropics than in the tropics. This global rectification effect, even its sign, still remains speculative, because it depends on the physical processes involved. Much work is needed to better understand this effect in more realistic settings especially in the coupled climate system.

APPENDIX A: ROSSBY WAVES AND TELECONNECTIONS

[76] Planetary-scale Rossby waves play a key role in the dynamic teleconnections in both the atmosphere and ocean. These waves can be identified in the alternating high- and low-pressure anomalies apparent in some atmospheric teleconnection patterns (Figure 7) including the atmospheric response to El Niño (see Figure 3). They are also crucial for the oceanic teleconnection in the interior ocean (Figure 10).

A1. Atmospheric Rossby Wave and Teleconnection

[77] Atmospheric Rossby waves conserve total vorticity (the rotation of the atmosphere and Earth) and have maximum amplitude in the upper troposphere. In the tropics, heating is balanced by vertical motion and strong divergence in the upper troposphere; the later is a source of vorticity, which generates Rossby waves [e.g., *Hoskins et al.*, 1977; *Hoskins and Karoly*, 1981]. Following *Sardeshmukh and Hoskins* [1985, 1988] and neglecting friction, the vorticity equation at a single level in the upper troposphere can be written as

$$\frac{\partial \zeta}{\partial t} + \mathbf{v}\cdot\nabla(\zeta + f) = -(\zeta + f)\nabla\cdot\mathbf{v}, \tag{A1}$$

where ζ (= $\partial v/\partial x - \partial u/\partial y$) is the vertical component of relative vorticity, t is time, $\mathbf{v} = (u, v)$ is the horizontal velocity, $f = 2\Omega \sin\phi$ is the Coriolis force, and $\nabla\cdot\mathbf{v}$ is the divergence (D). Partitioning the flow into a nondivergent and irrotational component, $\mathbf{v} = \mathbf{v}_\psi + \mathbf{v}_\chi$, the anomalous vorticity equation can be written as

$$\frac{\partial \zeta'}{\partial t} + \mathbf{U}\cdot\nabla\zeta' + \mathbf{v}'_\psi\cdot\nabla\overline{\zeta} = -(\overline{\zeta} + f)D' - \overline{D}\zeta' - \mathbf{v}'_\chi\cdot\nabla(\overline{\zeta} + f) - \overline{\mathbf{v}}_\chi\cdot\nabla\zeta' - \zeta'\nabla\cdot\mathbf{v}'_\psi - \zeta'\nabla\cdot\mathbf{v}'_\chi, \tag{A2}$$

where an overbar indicates the time mean and a prime indicates the departure from the mean; the mean irrotational flow is denoted as $\overline{\mathbf{v}}_\psi \equiv \mathbf{U} = (U, V)$. A stream function, ψ, can be defined for the irrotational flow, such that $u_\psi = -\partial\psi/\partial y$, $v_\psi = \partial\psi/\partial x$, and $\zeta = \nabla^2\Psi$. For large-scale flows the irrotational flow is usually dominant, while

the divergence flow is negligible except for the perturbation divergence (first term on the right-hand side of (A2)). In the atmosphere the mean flow is dominated by a zonal flow U. (More precisely, in the atmosphere, one should use the zonal average of the mean flow so that V vanishes [see *Hoskins and Karoly*, 1981]). Denoting $\beta = \partial f/\partial y$ and considering a small perturbation ψ', (A2) can be expressed as

$$\left(\frac{\partial}{\partial t} + U\frac{\partial}{\partial x}\right)\nabla^2\psi' + \frac{\partial\psi'}{\partial x}\left(\beta - \frac{\partial^2 U}{\partial y^2}\right) = \text{divergence forcing}, \tag{A3}$$

where the divergence terms on the right-hand side of (A1) or (A2) are specified as a forcing in (A3). Assuming that the perturbations are much smaller in scale than that of the background flow, a wave-type solution for (A3) of the form

$$\psi' = A\exp[i(kx + ly - \omega t)] \tag{A4}$$

is possible, where A is the amplitude of the perturbation, k and l are the zonal and meridional wave numbers, and ω is the frequency. Neglecting divergence forcing, using (A4) in (A3) yields the dispersion relationship for the free Rossby waves as

$$\omega = Uk - \left(\beta - \partial^2 U/\partial y^2\right)k/\left(k^2 + l^2\right). \tag{A5}$$

The propagation speed of individual waves is given by $c = (\omega/k,\ \omega/l)$, while wave energy, the key factor for climate anomalies, travels from the region of forcing with the group velocity $c_g = (\partial\omega/\partial k,\ \partial\omega/\partial l)$, representing the atmospheric teleconnection. For stationary waves, $\omega = c = 0$ (but $c_g \neq 0$), and (A5) can be written as

$$l = \pm\sqrt{(\beta - \partial^2 U/\partial y^2)/(U - k^2)}. \tag{A6}$$

When l is imaginary, the waves are evanescent; that is, they dissipate (no teleconnection) in the meridional direction as the exponential term in (A4) < 1, while waves propagate (as teleconnection) when l is real. Here l is imaginary where $U < 0$, i.e., in easterly winds, and when approaching the pole (or in some instances on the northern flank of the jet stream), where $\beta < \partial^2 U/\partial y^2$. Additional analyses suggest that the waves dissipate and/or are reflected when they approach the critical latitude ($U = c$), $U = 0$ for stationary waves, and will be refracted away from the pole [e.g., see *James*, 1995].

[78] *Hoskins and Karoly* [1981] considered only the first term on the right-hand side of (A2) a Rossby wave source. However, *Sardeshmukh and Hoskins* [1988] found that $\mathbf{v}'_\chi \cdot \nabla(\overline{\zeta} + f)$ is an especially effective source of Rossby waves, while the last two terms in (A2) generate Rossby waves via changes in the midlatitude storm track [*Ting and Held*, 1990]. With the inclusion of these additional source terms and using a realistic background state that includes longitudinal variations in U, many aspects of the observed atmospheric response to El Niño and teleconnection fit within the framework of single-level vorticity dynamics and Rossby wave dispersion.

A2. Oceanic Rossby Wave and Teleconnection

[79] The ocean has a Rossby deformation radius (a spatial scale beyond which rotation effect becomes important) of tens of kilometers, which is much smaller than the deformation radius of the atmosphere (thousands of kilometers) mainly because of the much weaker stratification in the ocean. For waves longer than the deformation radius, the divergence term on the right-hand side of (A1) becomes critically important. For large-scale, low-frequency oceanic variability the linearized vorticity equation can therefore be derived from (A2) by retaining only the first term on the right-land side as

$$\frac{\partial\zeta'}{\partial t} + \mathbf{U}\cdot\nabla\zeta' + \mathbf{v}'_\psi\cdot\nabla\overline{\zeta} + \left(\overline{\zeta} + f\right)D' = \text{vorticity forcing}, \tag{A7}$$

where the vorticity forcing due to wind or buoyancy is also added. The divergence can be obtained from the continuity equation and thermodynamic equation (such that (A7) becomes the so-called quasi-geostrophic equation [*Pedlosky*, 1987a]) and depends on the stratification and the stretching potential vorticity. Assuming the scale of the perturbation is much smaller than that of the mean flow and stratification, the oceanic disturbance can be approximated as

$$\psi' = A\exp[i(kx + ly + mz - \omega t)], \tag{A8}$$

where m is the vertical wave number. The dispersion relationship for free oceanic Rossby waves can therefore be derived from (A7) as

$$\omega = (Uk + Vl) - \left\{k\left[\beta - \frac{\partial^2}{\partial z^2}\left(\frac{f^2 U}{N^2}\right)\right] - l\frac{\partial^2}{\partial z^2}\left(\frac{f^2 V}{N^2}\right)\right\} \Big/ \left(k^2 + l^2 + L_m^{-2}\right). \tag{A9}$$

Here $N^2 > 0$ is the buoyancy frequency (which is proportional to the stratification), and $L_m = N/fm$ is the deformation radius corresponding to wave number m. The mean potential vorticity associated with the horizontal shear of the mean flow is also neglected relative to the stretching effect. In the absence of mean advection $\boldsymbol{U} = 0$ the dispersion relationship is reduced to $\omega = -\beta k/(k^2 + l^2 + L_m^{-2})$. One can show that the group velocity of the Rossby wave is westward for long waves of $k^2 + l^2 \ll L_m^{-2}$ but is eastward and much slower for short waves. These short eastward Rossby waves are arrested by mixing or trapped by advection to form the western boundary currents [*Pedlosky*, 1987a]. For long Rossby waves the dispersion relationship can be approximated as

$$\omega = (Uk + Vl) - \left\{k\left[\beta - \frac{\partial^2}{\partial z^2}\left(\frac{f^2 U}{N^2}\right)\right] - l\frac{\partial^2}{\partial z^2}\left(\frac{f^2 V}{N^2}\right)\right\}L_m^2 \tag{A10}$$

such that the wave becomes nondispersive (with the phase velocity equal to the group velocity $\mathbf{c} = \mathbf{c}_g$). If, furthermore,

the vertical structure of the mean flow is similar to the perturbation (A8), we have

$$\frac{\partial^2}{\partial z^2}\left(\frac{f^2U}{N^2}\right) \approx -\frac{f^2m^2}{N^2}U, \qquad \frac{\partial^2}{\partial z^2}\left(\frac{f^2V}{N^2}\right) \approx -\frac{f^2m^2}{N^2}V,$$

and therefore (A10) can be reduced to

$$\omega = -\beta L_m^2 k. \tag{A11}$$

Now the mean advection (Doppler shift) effect is canceled by the potential vorticity change associated with the mean flow. Consequently, Rossby waves propagate westward regardless of the mean flow. The mean thermocline circulation resembles closely the first baroclinic mode structure ($m = 1/H$) (H is the mean depth of the ocean). Therefore the first baroclinic wave is non-Doppler shifted and propagates westward (according to (A11)) to form the Sverdrup interior flow [*Anderson and Gill*, 1975]. In contrast, the higher baroclinic modes ($m = 2/H, 3/H \ldots$) tend to be advected by the mean thermocline flow (following (A10)) as advective modes [*Liu*, 1999]. These advective modes represent the ventilation processes of thermocline density anomalies. It is seen in (A10) that the mean meridional flow V is critical for the meridional propagation and, in turn, the ventilation and dynamic oceanic teleconnection. This is in contrast to the teleconnection in the atmosphere, where the meridional propagation is largely caused by the wave dispersion in the absence of mean meridional flow, as shown in (A5) and (A6).

[80] **ACKNOWLEDGMENTS.** Z. L. would like to thank J. Marotzke for a helpful discussion on the THC teleconnection and R. Zhang and P. Cessi for providing preprint figures. M. A. would like to acknowledge J. Scott at CDC who made some of the figures. Z. L. acknowledges support from NOAA-Clivar, DOE-CCPP, and NSF-ESH, while M. A. acknowledges support from NOAA-Clivar-Pacific.

[81] The Editor responsible for this paper was Henk Dijkstra. He thanks two anonymous technical reviewers and one anonymous cross-disciplinary reviewer.

REFERENCES

Adkins, J. F., K. McIntyre, and D. P. Schrag (2002), The salinity, temperature, and δ^{18}O of the glacial deep ocean, *Science*, *298*, 1769–1773.

Alexander, M. A. (1990), Simulation of the response of the North Pacific Ocean to the anomalous atmospheric circulation associated with El Niño, *Clim. Dyn.*, *5*, 53–65.

Alexander, M. A. (1992), Midlatitude atmosphere-ocean interaction during El Niño. part I: The North Pacific Ocean, *J. Clim.*, *5*, 944–958.

Alexander, M. A., C. Deser, and M. S. Timlin (1999), The reemergence of SST anomalies in the North Pacific Ocean, *J. Clim.*, *12*, 2419–2433.

Alexander, M. A., I. Bladé, M. Newman, J. R. Lanzante, N.-C. Lau, and J. D. Scott (2002), The atmospheric bridge: The influence of ENSO teleconnections on air-sea interaction over the global oceans, *J. Clim.*, *15*, 2205–2231.

Alexander, M. A., U. S. Bhatt, J. E. Walsh, M. S. Timlin, J. S. Miller, and J. D. Scott (2004a), The atmospheric response to realistic Arctic sea ice anomalies in an AGCM during winter, *J. Clim.*, *17*, 890–905.

Alexander, M. A., N.-C. Lau, and J. D. Scott (2004b), Broadening the atmospheric bridge paradigm: ENSO teleconnections to the North Pacific in summer and to the tropical west Pacific-Indian oceans over the seasonal cycle, in *Earth's Climate: The Ocean-Atmosphere Interaction*, *Geophys. Monogr. Ser.*, vol. 147, edited by C. Wang, S.-P. Xie, and J. A. Carton, pp. 85–104, AGU, Washington, D. C.

Alley, R. B., E. J. Brook, and S. Anadakrikhnan (2002), A northern lead in the orbital band: North-south phasing of ice-age events, *Quat. Sci. Rev.*, *21*, 431–441.

Ambaum, M. H. P., B. J. Hoskins, and D. B. Stephenson (2001), Arctic Oscillation or North Atlantic Oscillation?, *J. Clim.*, *14*, 3495–3507.

Anderson, D. L. T., and A. E. Gill (1975), Spin-up of a stratified ocean, with applications to upwelling, *Deep Sea Res. Oceanogr. Abstr.*, *24*, 583–596.

Ångström, A. (1935), Teleconnections of climate changes in present time, *Geogr. Ann.*, *17*, 242–258.

Archer, D., A. Winguth, D. Lea, and N. Mahowald (2000), What caused the glacial/interglacial atmospheric pCO_2 cycles?, *Rev. Geophys.*, *38*, 159–189.

Baldwin, M. P., and T. J. Dunkerton (1999), Propagation of the Arctic Oscillation from the stratosphere to the troposphere, *J. Geophys. Res.*, *104*, 30,937–30,946.

Baldwin, M. P., and T. J. Dunkerton (2001), Stratospheric harbingers of anomalous weather regimes, *Science*, *294*, 581–584.

Barlow, M., S. Nigam, and E. H. Berbery (2001), ENSO, Pacific decadal variability, and U.S. summertime precipitation, drought, and stream flow, *J. Clim.*, *14*, 2105–2128.

Barnett, T., D. W. Pierce, M. Latif, D. Dommonget, and R. Saravana (1999), Interdecadal interactions between the tropics and the midlatitudes in the Pacific basin, *Geophys. Res. Lett.*, *26*, 615–618.

Barnston, A. G., and R. E. Livezey (1987), Classification, seasonality and persistence of low-frequency atmospheric circulation patterns, *Mon. Weather Rev.*, *115*, 1083–1126.

Barsugli, J. J., and P. D. Sardeshmukh (2002), Global atmospheric sensitivity to tropical SST anomalies throughout the Indo-Pacific basin, *J. Clim.*, *15*, 3427–3442.

Bjerknes, J. (1966), A possible response of the atmospheric Hadley circulation to equatorial anomalies of ocean temperatures, *Tellus*, *18*, 820–829.

Bjerknes, J. (1969), Atmospheric teleconnections from the equatorial Pacific, *Mon. Weather Rev.*, *97*, 163–172.

Black, R. X. (2002), Stratospheric forcing of surface climate in the Arctic Oscillation, *J. Clim.*, *15*, 268–277.

Bladé, I. (1999), The influence of midlatitude ocean-atmosphere coupling on the low-frequency variability of a GCM. Part II: Interannual variability induced by tropical SST forcing, *J. Clim.*, *12*, 21–45.

Boer, G. J., and B. Yu (2003a), Dynamical aspects of climate sensitivity, *Geophys. Res. Lett.*, *30*(3), 1135, doi:10.1029/2002GL016549.

Boer, G. J., and B. Yu (2003b), Climate sensitivity and response, *Clim. Dyn.*, *20*, 415–429.

Borges, M., and P. D. Sardeshmukh (1995), Barotropic Rossby wave dynamics of zonally varying upper-level flows during northern winter, *J. Atmos. Sci.*, *52*, 3779–3796.

Boyle, E. A., and L. D. Keigwin (1987), North Atlantic thermohaline circulation during the past 20,000 years linked to high-latitude surface temperature, *Nature*, *330*, 35–40.

Branstator, G. (1983), Horizontal energy propagation in a barotropic atmosphere with meridional and zonal structure, *J. Atmos. Sci.*, *40*, 1689–1708.

Branstator, G. (1995), Organization of storm track anomalies by recurring low-frequency circulation anomalies, *J. Atmos. Sci.*, *52*, 207–226.

Branstator, G. (2002), Circumglobal teleconnections, the jet stream waveguide, and the North Atlantic Oscillation, *J. Clim.*, *15*, 1893–1910.

Broecker, W. S. (1998), Paleocean circulation during the last deglaciation: A bipolar seesaw?, *Paleoceanography*, *13*, 119–121.
Broecker, W. S., and G. H. Denton (1989), The role of ocean-atmosphere reorganizations in glacial cycles, *Geochim. Cosmochim. Acta*, *53*, 2465–2501.
Bryan, F. (1986), High-latitude salinity effects and interhemispheric thermohaline circulations, *Nature*, *323*, 301–304.
Bryan, F. (1987), Parameter sensitivity of primitive equation ocean general circulation models, *J. Phys. Oceanogr.*, *14*, 666–673.
Bryan, K. (1963), A numerical investigation of a non-linear model of a wind-driven ocean, *J. Atmos. Sci.*, *20*, 594–606.
Bryden, H. L., D. H. Roemmich, and J. A. Church (1991), Oceanic heat transport across 24°N in the Pacific, *Deep Sea Res., Part I*, *38*, 297–324.
Cai, M. (2005), Dynamical amplification of polar warming, *Geophys. Res. Lett.*, *32*, L22710, doi:10.1029/2005GL024481.
Cane, M. A. (1998), A role for the tropical Pacific, *Science*, *282*, 59–61.
Cane, M. A., and E. S. Sarachik (1976), Forced baroclinic ocean motions. I. The linear equatorial unbounded case, *J. Mar. Res.*, *34*, 629–665.
Cane, M. A., and E. S. Sarachik (1977), Forced baroclinic ocean motions. II. The linear equatorial bounded case, *J. Mar. Res.*, *35*, 395–432.
Capotondi, A., and M. A. Alexander (2001), Rossby waves in the tropical North Pacific and their role in decadal thermocline variability, *J. Phys. Oceanogr.*, *31*, 3496–3515.
Capotondi, A., M. A. Alexander, C. Deser, and M. McPhaden (2005), Anatomy and decadal evolution of the Pacific subtropical cells (STCs), *J. Clim.*, *18*, 3739–3758.
Cassou, C., L. Terray, J. W. Hurrell, and C. Deser (2004), North Atlantic winter climate regimes: Spatial asymmetry, stationarity with time, and oceanic forcing, *J. Clim.*, *17*, 1055–1068.
Cessi, P., and S. Louazel (2001), Decadal oceanic response to stochastic wind forcing, *J. Phys. Oceanogr.*, *31*, 3020–3029.
Cessi, P. G., R. Ierley, and W. R. Young (1987), A model of the inertial recirculation driven by potential vorticity anomalies, *J. Phys. Oceanogr.*, *17*, 1640–1652.
Cessi, P., K. Bryan, and R. Zhang (2004), Global seiching of thermocline waters between the Atlantic and the Indian-Pacific Ocean basins, *Geophys. Res. Lett.*, *31*, L04302, doi:10.1029/2003GL019091.
Chang, E. K. M. (1995), The influence of Hadley circulation intensity changes on extratropical climate in an idealized model, *J. Atmos. Sci.*, *52*, 2006–2024.
Chang, E. K. M. (1998), Poleward-propagating angular momentum perturbations induced by zonally symmetric heat sources in the tropics, *J. Atmos. Sci.*, *55*, 2229–2248.
Charney, J. G. (1955), The Gulf Stream as an inertial boundary layer, *Proc. Natl. Acad. Sci. U. S. A.*, *41*, 731–740.
Chelton, D. B., and R. E. Davis (1982), Monthly mean sea level variability along the west coast of North America, *J. Phys. Oceanogr.*, *12*, 757–784.
Chelton, D. B., and M. G. Schlax (1996), Global observations of oceanic Rossby waves, *Science*, *272*, 234–238.
Chen, L.-G., and W. K. Dewar (1993), Intergyre communication in a three-layer model, *J. Phys. Oceanogr.*, *23*, 855–878.
Chen, T.-C., and M. C. Yen (1993), Interannual variation of summertime stationary eddies, *J. Clim.*, *6*, 2263–2277.
Chiang, J. C. H., and C. M. Bitz (2005), Influence of high latitude ice cover on the marine Intertropical Convergence Zone, *Clim. Dyn.*, *25*, 477–496, doi:10.1007/s00382-005-0040-5.
Chiang, J. C. H., and D. J. Vimont (2004), Analogous Pacific and Atlantic meridional modes of tropical atmosphere-ocean variability, *J. Clim.*, *17*, 4143–4158.
Chiang, J. C., M. Biasutti, and D. S. Battisti (2003), Sensitivity of the Atlantic Intertropical Convergence Zone to Last Glacial Maximum boundary conditions, *Paleoceanography*, *18*(4), 1094, doi:10.1029/2003PA000916.
Clarke, A. J., and A. Levedev (1997), Interannual and decadal changes in equatorial wind stress in the Atlantic, Indian, and Pacific oceans and the eastern ocean coastal response, *J. Clim.*, *10*, 1722–1729.
Clement, A., and R. Seager (1999), Climate and the tropical oceans, *J. Clim.*, *12*, 3383–3401.
Clement, A., R. Seager, and M. Cane (1999), Orbital controls on ENSO and the tropical climate, *Paleoceanography*, *14*, 441–456.
Cook, K. (2001), A Southern Hemisphere wave response to ENSO with implications for southern Africa precipitation, *J. Atmos. Sci.*, *58*, 2146–2162.
Cook, K. (2004), Hadley circulation dynamics: Seasonality and the role of the continents, in *The Hadley Circulation: Present*, *Past*, *and Future*, *Adv. Global Change Res.*, vol. 21, edited by H. F. Diaz and R. S. Bradley, pp. 61–84, Springer, New York.
Cubasch, U., et al. (2001), Projections of future climate change, in *Climate Change 2001: The Scientific Basis*, edited by J. T. Houghton et al., chap. 9, pp. 525–582, Cambridge Univ. Press, New York.
Czaja, A., and C. Frankignoul (2002), Observed impact of North Atlantic SST anomalies on the North Atlantic Oscillation, *J. Clim.*, *15*, 606–623.
Czaja, A., P. van der Vaart, and J. Marshall (2002), A diagnostic study of the role of remote forcing in tropical Atlantic variability, *J. Clim.*, *15*, 3280–3290.
Defant, A. (1941), Quantitative Untersuchungen zur Statik und Dynamik des Atlantischen Ozeans: Die relativ Topographie einzelner Druckflachen im Atlantischen Ozean, *Wiss. Ergeb. Dtsch. Atl. Exped. Meteor 1925–1927*, *6*, 191–260.
Deser, C. (2000), On the teleconnectivity of the "Arctic Oscillation", *Geophys. Res. Lett.*, *27*, 779–782.
Deser, C., M. A. Alexander, and M. S. Timlin (1996), Upper-ocean thermal variations in the North Pacific during 1970–91, *J. Clim.*, *9*, 1840–1855.
Deser, C., J. E. Walsh, and M. S. Timlin (2000), Arctic sea ice variability in the context of recent atmospheric circulation trends, *J. Clim.*, *13*, 617–633.
Deser, C., G. Magnusdottir, R. Saravanan, and A. Phillips (2004a), The effect of North Atlantic SST and sea ice anomalies on the winter circulation in CCM3. part II: Direct and indirect components of the response, *J. Clim.*, *17*, 877–889.
Deser, C., A. S. Phillips, and J. W. Hurrell (2004b), Pacific interdecadal climate variability: Linkages between the tropics and the North Pacific during boreal winter since 1900, *J. Clim.*, *17*, 3109–3124.
DeWeaver, E., and S. Nigam (2000a), Do stationary waves drive the zonal-mean jet anomalies of the northern winter?, *J. Clim.*, *13*, 2160–2176.
DeWeaver, E., and S. Nigam (2000b), Zonal-eddy dynamics of the North Atlantic Oscillation, *J. Clim.*, *13*, 3893–3914.
DeWeaver, E., and S. Nigam (2002), Linearity in ENSO's atmospheric response, *J. Clim.*, *15*, 2446–2461.
DeWeaver, E., and S. Nigam (2004), On the forcing of ENSO teleconnections by anomalous heating and cooling, *J. Clim.*, *17*, 3225–3235.
Dommonget, D., and M. Latif (2002), A cautionary note on the interpretation of EOFs, *J. Clim.*, *15*, 216–225.
Dong, B.-W., and R. T. Sutton (2002), Adjustment of the coupled ocean-atmosphere system to a sudden change in the thermohaline circulation, *Geophys. Res. Lett.*, *29*(15), 1728, doi:10.1029/2002GL015229.
Drevillon, M., C. Cassou, and L. Terray (2003), Model study of the North Atlantic region atmospheric response to autumn tropical Atlantic sea-surface-temperature anomalies, *Q. J. R. Meteorol. Soc.*, *129*, 2591–2611.
Duplessy, J. C., et al. (1988), Deepwater source variations during the last climate cycle and their impact on the global deepwater circulation, *Paleoceanography*, *3*, 343–360.
Edmon, H. J., Jr., B. J. Hoskins, and M. E. McIntyre (1980), Eliassen-Palm cross sections for the troposphere, *J. Atmos. Sci.*, *37*, 2600–2616.

Ellis, H. (1751), A letter to the Rev. Dr. Hales, F. R. S. from Captain Henry Ellis, F. R. S. dated Jan. 7, 1950–51, at Cape Monte Africa, Ship Earl of Halifax, *Philos. Trans. R. Soc. London*, *47*, 211–214.

Enfield, D. B., and J. S. Allen (1980), On the structure and dynamics of monthly mean sea level anomalies along the Pacific coast of North and South America, *J. Phys. Oceanogr.*, *10*, 557–588.

Evans, M. N., M. A. Cane, D. P. Schrag, A. Kaplan, B. K. Linsley, R. Villalba, and G. M. Wellington (2001), Support for tropically-driven Pacific decadal variability based on paleoproxy evidence, *Geophys. Res. Lett.*, *28*, 3689–3692.

Fine, R. A., W. H. Peterson, and H. G. Ostlund (1987), The penetration of the tritium into the tropical Pacific, *J. Phys. Oceanogr.*, *17*, 553–564.

Francois, R., M. A. Altabet, E.-F. Yu, D. M. Sigman, M. P. Bacon, M. Frank, G. Bohrmann, G. Bareille, and L. D. Labeyrie (1998), Contribution of Southern Ocean surface water stratification to low atmospheric CO_2 concentrations during the last glacial period, *Nature*, *389*, 929–935.

Garreaud, R. D., and D. S. Battisti (1999), Interannual (ENSO) and interdecadal (ENSO-like) variability in the Southern Hemisphere tropospheric circulation, *J. Clim.*, *12*, 2113–2123.

Gill, A. E. (1980), Some simple solutions for heat-induced tropical circulation, *Q. J. R. Meteorol. Soc.*, *106*, 447–462.

Glantz, M. H., R. W. Katz, and N. Nicholls (Eds.) (1991), *Teleconnections Linking Worldwide Climate Anomalies: Scientific Basis and Societal Impact*, 535 pp., Cambridge Univ. Press, New York.

Gong, D., and S. Wang (1999), Definition of Antarctic Oscillation index, *Geophys. Res. Lett.*, *26*, 459–462.

Graham, N. E., and T. P. Barnett (1987), Sea surface temperature, surface wind divergence and convection over the tropical oceans, *Science*, *238*, 657–659.

Graham, N. E., T. P. Barnett, R. Wilde, M. Ponater, and S. Schubert (1994), On the roles of tropical and midlatitude SSTs in forcing annual to interdecadal variability in the winter Northern Hemisphere circulation, *J. Clim.*, *7*, 1416–1442.

Gu, D., and S. G. H. Philander (1997), Interdecadal climate fluctuations that depend on exchanges between the tropics and the extratropics, *Science*, *275*, 805–807.

Hall, M. M., and H. L. Bryden (1982), Direct estimates and mechanisms of ocean heat transport, *Deep Sea Res., Part A*, *29*, 339–359.

Hall, N. M. J., and J. Derome (2000), Transients, nonlinearity, and eddy feedback in the remote response to El Niño, *J. Atmos. Sci.*, *57*, 3992–4007.

Hall, N. M. J., J. Derome, and H. Lin (2001), The extratropical signal generated by a midlatitude SST anomaly. part I: Sensitivity at equilibrium, *J. Clim.*, *14*, 2035–2053.

Hartmann, D. L., and F. Lo (1998), Wave-driven zonal flow vacillation in the Southern Hemisphere, *J. Atmos. Sci.*, *55*, 1303–1315.

Hastenrath, S. (1982), On meridional heat transports in the world ocean, *J. Phys. Oceanogr.*, *2*, 922–927.

Held, I. (2001), The partitioning of the poleward energy transport between the tropical ocean and atmosphere, *J. Atmos. Sci.*, *58*, 943–948.

Held, I. M., and A. Y. Hou (1980), Nonlinear axially symmetric circulations in a nearly inviscid atmosphere, *J. Atmos. Sci.*, *37*, 515–533.

Held, I. M., and I.-S. Kang (1987), Barotropic models of the extratropical response to El Niño, *J. Atmos. Sci.*, *44*, 3576–3586.

Held, I. M., S. W. Lyons, and S. Nigam (1989), Transients and the extratropical response to El Niño, *J. Atmos. Sci.*, *46*, 163–174.

Hildebrandsson, H. H. (1897), Quelque recherches sur les entres d'action de l'atmosphere, *K. Sven. Vetenskapsakad. Handl.*, *29*, 1–33.

Hoerling, M. P., and A. Kumar (2003), The perfect ocean for drought, *Science*, *299*, 691–694.

Hoerling, M. P., and M. Ting (1994), Organization of extratropical transients during El Niño, *J. Clim.*, *7*, 745–766.

Hoerling, M. P., A. Kumar, and M. Zhong (1997), El Niño, La Niña, and the nonlinearity of their teleconnections, *J. Clim.*, *10*, 1769–1786.

Hoerling, M. P., A. Kumar, and T.-Y. Xu (2001a), Robustness of the nonlinear atmospheric response to opposite phases of ENSO, *J. Clim.*, *14*, 1277–1293.

Hoerling, M. P., J. Hurrell, and T. Xu (2001b), Tropical origins for North Atlantic climate change, *Science*, *292*, 90–92.

Hoerling, M. P., J. W. Hurrell, T. Xu, G. T. Bates, and A. S. Phillips (2004), Twentieth century North Atlantic climate change. part II: Understanding the effect of Indian Ocean warming, *Clim. Dyn.*, *23*, 391–405.

Honda, M., H. Nakamura, J. Ukita, I. Kousaka, and K. Takeuchi (2001), Interannual seesaw between the Aleutian and Icelandic lows. part I: Seasonal dependence and life cycle, *J. Clim.*, *14*, 1029–1042.

Honda, M., Y. Kushnir, H. Nakamura, S. Yamane, and S. E. Zebiak (2005), Formation, mechanisms, and predictability of the Aleutian-Icelandic low seesaw in ensemble AGCM simulations, *J. Clim.*, *18*, 1423–1434.

Horel, J. D., and J. M. Wallace (1981), Planetary-scale atmospheric phenomena associated with the interannual variability of sea surface temperature in the equatorial Pacific, *Mon. Weather Rev.*, *109*, 813–829.

Hoskins, B. J., and T. Ambrizzi (1993), Rossby wave propagation on a realistic longitudinally varying flow, *J. Atmos. Sci.*, *50*, 1661–1671.

Hoskins, B. J., and D. J. Karoly (1981), The steady linear response of a spherical atmosphere to thermal and orographic forcing, *J. Atmos. Sci.*, *38*, 1179–1196.

Hoskins, B. J., A. J. Simmons, and D. G. Andrews (1977), Energy dispersion in a barotropic atmosphere, *Q. J. R. Meteorol. Soc.*, *103*, 553–568.

Hoskins, B. J., I. N. James, and G. H. White (1983), The shape, propagation and mean-flow interaction of large-scale weather systems, *J. Atmos. Sci.*, *40*, 1595–1612.

Huang, B. Y., and Z. Liu (1999), Pacific subtropical-tropical thermocline water exchange in the National Centers for Environmental Prediction ocean model, *J. Geophys. Res.*, *104*, 11,065–11,076.

Huang, R. X. (1999), Mixing and energetics of the oceanic thermohaline circulation, *J. Phys. Oceanogr.*, *29*, 727–746.

Huang, R. X., M. Cane, N. Naik, and P. Goodman (2000), Global adjustment of the thermocline in response to deepwater formation, *Geophys. Res. Lett.*, *27*, 759–762.

Hughes, T., and A. J. Weaver (1994), Multiple equilibria of an asymmetric two-basin model, *J. Phys. Oceanogr.*, *24*, 619–637.

Hurrell, J. W., Y. Kushnir, G. Ottersen, and M. Visbeck, (Eds.) (2003), *The North Atlantic Oscillation: Climate Significance and Environmental Impact*, *Geophys. Monogr. Ser.*, vol. 134, 279 pp., AGU, Washington, D. C.

Inui, T., A. Lazar, P. Malanotte-Rizzoli, and A. Busalacchi (2002), Wind stress effects on subsurface pathways from the subtropical to tropical Atlantic, *J. Phys. Oceanogr.*, *32*, 2257–2276.

Jacobs, G. A., H. E. Hurlburt, J. C. Kindle, E. J. Metzger, J. L. Mitchell, W. J. Teague, and A. G. Wallcraft (1994), Decade-scale trans-Pacific propagation and warming effects of an El Niño anomaly, *Nature*, *370*, 360–363.

James, I. N. (1995), *Introduction to Circulating Atmospheres*, 422 pp., Cambridge Univ. Press, New York.

James, I. N. (2003), Hadley circulation, in *Encyclopedia of Atmospheric Sciences*, edited by J. R. Holton et al., pp. 919–929, Elsevier, New York.

Jayne, S. R., and J. Marotzke (2001), The dynamics of ocean heat transport variability, *Rev. Geophys.*, *39*, 385–417.

Johnson, G., and M. McPhaden (1999), Interior pycnocline flow from the subtropical to the equatorial Pacific Ocean, *J. Phys. Oceanogr.*, *29*, 3073–3089.

Johnson, H. L., and D. P. Marshall (2002), A theory for the surface Atlantic response to thermohaline variability, *J. Phys. Oceanogr.*, *32*, 1121–1132.

Johnson, H. L., and D. P. Marshall (2004), Global teleconnections of meridional overturning circulation anomalies, *J. Phys. Oceanogr.*, *34*, 1702–1722.

Kalnay, E., et al. (1996), The NCEP/NCAR 40-year reanalysis project, *Bull. Am. Meteorol. Soc.*, *77*, 437–471.

Karoly, D. J. (1990), The role of transient eddies in low-frequency zonal variations of the Southern Hemisphere circulation, *Tellus, Ser. A*, *42*, 41–50.

Kasahara, A., and P. L. D. Silva Dias (1986), Response of planetary waves to stationary tropical heating in a global atmosphere with meridional and vertical shear, *J. Atmos. Sci.*, *43*, 1893–1911.

Kawase, M. (1987), Establishment of deep ocean circulation driven by deep water production, *J. Phys. Oceanogr.*, *17*, 2294–2317.

Keigwin, L. D., W. B. Curry, S. J. Lehman, and S. Johnsen (1994), The role of the deep ocean in North Atlantic climate change between 70 and 130 kyr ago, *Nature*, *371*, 323–326.

Keith, D. W. (1995), Meridional energy transport, uncertainty in zonal means, *Tellus, Ser. A*, *47*, 30–44.

Kidson, J. W. (1988), Interannual variations in the Southern Hemisphere circulation, *J. Clim.*, *1*, 1177–1198.

Kiladis, G. N., and K. M. Weickmann (1992), Extratropical forcing of tropical Pacific convection during northern winter, *Mon. Weather Rev.*, *120*, 1924–1938.

Kistler, R., et al. (2001), The NCEP-NCAR 50-year reanalysis: Monthly means CD-ROM and documentation, *Bull. Am. Meteorol. Soc.*, *82*, 247–268.

Kleeman, R., J. P. McCreary, and B. A. Klinger (1999), A mechanism for the decadal variation of ENSO, *Geophys. Res. Lett.*, *26*, 1743–1747.

Klein, S. A., D. L. Hartmann, and J. R. Norris (1995), On the relationships among low-cloud structure, sea surface temperature and atmospheric circulation in the summertime northeast Pacific, *J. Clim.*, *8*, 1140–1155.

Klein, S. A., B. J. Soden, and N.-C. Lau (1999), Remote sea surface variations during ENSO: Evidence for a tropical atmospheric bridge, *J. Clim.*, *12*, 917–932.

Klinger, B. A., and J. Marotzke (1999), Behavior of double hemisphere thermohaline flows in a single basin, *J. Phys. Oceanogr.*, *29*, 382–399.

Klinger, B. A., and J. Marotzke (2000), Meridional heat transport by the subtropical cell, *J. Phys. Oceanogr.*, *30*, 696–705.

Knorr, G., and G. Lohmann (2003), Southern Ocean origin for the resumption of Atlantic thermohaline circulation during deglaciation, *Nature*, *424*, 522–536.

Kok, C. J., and J. D. Opsteegh (1985), Possible causes of anomalies in seasonal mean circulation patterns during the 1982–83 El Nino event, *J. Atmos. Sci.*, *42*, 677–694.

Kosaka, Y., and H. Nakamura (2007), Structure and dynamics of the summertime Pacific-Japan (PJ) teleconnection pattern, *Q. J. R. Meteorol. Soc.*, in press.

Kushnir, Y., W. A. Robinson, I. Bladé, N. M. J. Hall, S. Peng, and R. Sutton (2002), Atmospheric response to extratropical SST anomalies: Synthesis and evaluation, *J. Clim.*, *15*, 2205–2231.

Latif, M., and T. Barnett (1994), Causes of decadal climate variability over the North Pacific and North America, *Science*, *266*, 634–637.

Lau, K.-M., and L. Peno (1992), Dynamics of atmospheric teleconnections during the northern summer, *J. Clim.*, *5*, 140–158.

Lau, K.-M., and H. Weng (2002), Recurrent teleconnection patterns linking summertime precipitation variability over east Asia and North America, *J. Meteorol. Soc. Jpn.*, *80*, 1129–1147.

Lau, N. C. (1988), Variability of the observed midlatitude storm tracks in relation to low-frequency changes in the circulation pattern, *J. Atmos. Sci.*, *45*, 2718–2743.

Lau, N. C., and M. J. Nath (1994), A modeling study of the relative roles of tropical and extratropical SST anomalies in the variability of the global atmosphere-ocean system, *J. Clim.*, *7*, 1184–1207.

Lau, N.-C., and M. J. Nath (1996), The role of the "atmospheric bridge" in linking tropical Pacific ENSO events to extratropical SST anomalies, *J. Clim.*, *9*, 2036–2057.

Lau, N.-C., and M. J. Nath (2001), Impact of ENSO on SST variability in the North Pacific and North Atlantic: Seasonal dependence and role of extratropical air-sea coupling, *J. Clim.*, *14*, 2846–2866.

Lau, N.-C., and M. J. Nath (2004), Coupled GCM simulation of atmosphere-ocean variability associated with zonally asymmetric SST changes in the tropical Indian Ocean, *J. Clim.*, *17*, 245–265.

Lee, T., and I. Fukumori (2003), Interannual-to-decadal variations of tropical-subtropical exchange in the Pacific Ocean: Boundary vs. interior pycnocline transports, *J. Clim.*, *16*, 4022–4042.

Lenz, E. (1845), Bermerkungen bei die Temperatur des Weltmeeres in verschiedenen Tiefen, *Bull. Cl. Phys. Math. Acad. Impetiale Sci. St. Petersbourg*, *5*, 67–74.

Lim, H., and C. P. Chang (1986), Generation of internal- and external-mode motions from internal heating: Effects of vertical shear and damping, *J. Atmos. Sci.*, *43*, 948–957.

Limpasuvan, V., and D. L. Hartmann (1999), Eddies and the annular modes of climate variability, *Geophys. Res. Lett.*, *26*, 3133–3136.

Limpasuvan, V., and D. L. Hartmann (2000), Wave-maintained annular modes of climate variability, *J. Clim.*, *13*, 4414–4429.

Lin, H., and J. Derome (2004), Nonlinearity of the extratropical response to tropical forcing, *J. Clim.*, *17*, 2597–2608.

Lindzen, R. S. (1990), *Dynamics in Atmospheric Physics*, 310 pp., Cambridge Univ. Press, New York.

Lindzen, R. S. (1994), Climate dynamics and global change, *Annu. Rev. Fluid Mech.*, *26*, 353–378.

Lindzen, R. S., and A. V. Hou (1988), Hadley circulations for zonally averaged heating centered off the equator, *J. Atmos. Sci.*, *45*, 2416–2427.

Liu, Z. (1999), Forced planetary wave response in a thermocline gyre, *J. Phys. Oceanogr.*, *29*, 1036–1055.

Liu, Z. (2002), How long is the memory of tropical ocean dynamics?, *J. Clim.*, *15*, 3518–3522.

Liu, Z. (2003), Tropical ocean decadal variability and the resonance of planetary wave basin modes: I: Theory, *J. Clim.*, *16*, 1539–1550.

Liu, Z. (2006), Glacial thermohaline and climate: Is it driven from the north or south?, *Adv. Atmos. Sci.*, *23*, 199–206.

Liu, Z., and B. Huang (1998), Why is there a tritium maximum in the central equatorial Pacific thermocline, *J. Phys. Oceanogr.*, *28*, 1527–1533.

Liu, Z., and G. Philander (2001), Tropical-extratropical oceanic exchange pathways, in *Ocean Circulation and Climate: Observing and Modeling the Global Ocean*, edited by G. Siedler, J. Church, and J. Gould, pp. 247–254, Elsevier, New York.

Liu, Z., and S. Shin (1999), On thermocline ventilation of active and passive tracers, *Geophys. Res. Lett.*, *26*, 357–360.

Liu, Z., and S. P. Xie (1994), Equatorward propagation of coupled air-sea disturbances with application to the annual cycle of the eastern tropical Pacific, *J. Atmos. Sci.*, *51*, 3807–3822.

Liu, Z., and H. Yang (2003), Extratropical control of tropical climate, the atmospheric bridge and oceanic tunnel, *Geophys. Res. Lett.*, *30*(5), 1230, doi:10.1029/2002GL016492.

Liu, Z., S. G. H. Philander, and R. C. Pacanowski (1994), A GCM study of the tropical-subtropical upper-ocean circulation, *J. Phys. Oceanogr.*, *24*, 2606–2623.

Liu, Z., L. Wu, and E. Bayler (1999a), Rossby wave–coastal Kelvin wave interaction in the extratropics. I: Low frequency adjustment in a closed basin, *J. Phys. Oceanogr.*, *29*, 2383–2404.

Liu, Z., L. Wu, and H. Hurlburt (1999b), Rossby wave–coastal Kelvin wave interaction in the extratropics. II: Formation of island circulation, *J. Phys. Oceanogr*, *29*, 2405–2418.

Liu, Z., S. Shin, B. Otto-Bliesner, J. E. Kutzbach, E. C. Brady, and D. Lee (2002), Tropical cooling at the Last Glacial Maximum

and extratropical ocean ventilation, *Geophys. Res. Lett.*, *29*(10), 1409, doi:10.1029/2001GL013938. (Correction, *Geophys. Res. Lett.*, *30*(3), 1104, doi:10.1029/2002GL016795, 2003.)

Liu, Z., E. Brady, and J. Lynch-Steiglitz (2003), Global ocean response to orbital forcing in the Holocene, *Paleoceanography*, *18*(2), 1041, doi:10.1029/2002PA000819.

Liu, Z., S. I. Shin, R. S. Webb, W. Lewis, and B. L. Otto-Bliesner (2005), Atmospheric CO_2 forcing on glacial thermohaline circulation and climate, *Geophys. Res. Lett.*, *32*, L02706, doi:10.1029/2004GL021929.

Lorenz, D. J., and D. L. Hartmann (2001), Eddy-zonal flow feedback in the Southern Hemisphere, *J. Atmos. Sci.*, *58*, 3312–3327.

Lorenz, D. J., and D. L. Hartmann (2003), Eddy-zonal flow feedback in the Northern Hemisphere, *J. Clim.*, *16*, 1212–1227.

Lu, P., and J. P. McCreary (1995), Influence of the ITCZ on the flow of the thermocline water from the subtropical to the equatorial Pacific Ocean, *J. Phys. Oceanogr.*, *25*, 3076–3088.

Lu, P., J. P. McCreary, and B. A. Klinger (1998), Meridional circulation cells and the source waters of the Pacific equatorial undercurrent, *J. Phys. Oceanogr.*, *28*, 62–83.

Luksch, U., and H. von Storch (1992), Modeling the low-frequency sea surface temperature variability in the North Pacific, *J. Clim.*, *5*, 893–906.

Luo, J. J., and T. Yamagata (2001), Long-term El Niño–Southern Oscillation (ENSO)-like variation with special emphasis on the South Pacific, *J. Geophys. Res.*, *106*, 22,211–22,227.

Luyten, J. R., J. Pedlosky, and H. Stommel (1983), The ventilated thermocline, *J. Phys. Oceanogr.*, *13*, 292–309.

Lynch-Steiglitz, J. (2004), Hemispheric asynchrony of abrupt climate change, *Science*, *304*, 1919–1920.

Lysne, J., P. Chang, and B. Giese (1997), Impact of the extratropical Pacific on equatorial variability, *Geophys. Res. Lett.*, *24*, 2589–2592.

Macdonald, A., and C. Wunsch (1996), An estimate of global ocean circulation and heat fluxes, *Nature*, *382*, 436–439.

Malanotte-Rizzoli, P., K. Hedstrom, H. Arango, and D. B. Haidvogel (2000), Water mass pathways between the subtropical and tropical ocean in a climatological simulation of the North Atlantic Ocean circulation, *Dyn. Atmos. Oceans*, *32*, 331–371.

Manabe, S., and R. Stouffer (1994), Multiple-century responses of a coupled ocean-atmosphere model to an increase of atmospheric carbon dioxide, *J. Clim.*, *7*, 5–23.

Mantua, N. J., S. R. Hare, Y. Zhang, J. M. Wallace, and R. Francis (1997), A Pacific interdecadal climate oscillation with impacts on salmon production, *Bull. Am. Meteorol. Soc.*, *78*, 1069–1079.

Markgraf, V. (Ed.) (2001), *Interhemispheric Climate Linkages*, 454 pp., Elsevier, New York.

Marotzke, J. (2000), Abrupt climate change and thermohaline circulation: Mechanisms and predictability, *Proc. Natl. Acad. Sci. U. S. A.*, *97*, 1347–1350.

Marotzke, J., and B. A. Klinger (2000), The dynamics of equatorially asymmetric thermohaline circulations, *J. Phys. Oceanogr.*, *30*, 955–970.

Marotzke, J., and J. R. Scott (1999), Convective mixing and thermohaline circulation, *J. Phys. Oceanogr.*, *29*, 2962–2970.

Marotzke, J., P. Welander, and J. Willebrand (1988), Instability and multiple steady states in a meridional-plane model of the thermohaline circulation, *Tellus, Ser. A*, *40*, 162–172.

McCreary, J. P., and P. Lu (1994), Interaction between the subtropical and equatorial ocean circulations: The subtropical cell, *J. Phys. Oceanogr.*, *24*, 466–497.

McPhaden, M. J., and D. Zhang (2002), Slowdown of the meridional over turning circulation in the upper Pacific Ocean, *Nature*, *415*, 603–608.

Miller, A. J., W. B. White, and D. R. Cayan (1997), North Pacific thermocline variations on ENSO timescales, *J. Clim.*, *27*, 2023–2039.

Miller, R. (1997), Tropical thermostats and low cloud cover, *J. Clim.*, *10*, 409–440.

Mo, K. C., and R. E. Livezey (1986), Tropical-extratropical geopotential height teleconnections during Northern Hemisphere winter, *Mon. Weather Rev.*, *114*, 2488–2515.

Mo, K. C., and G. H. White (1985), Teleconnections in the Southern Hemisphere, *Mon. Weather Rev.*, *113*, 22–37.

Munk, W., and C. Wunsch (1998), Abyssal recipes II: Energetics of tidal and wind mixing, *Deep Sea Res., Part I*, *45*, 1976–2009.

Murtugudde, R., J. Beauchamp, C. R. McClain, M. Lewis, and A. J. Busalacchi (2002), Effects of penetrative radiation on the upper tropical ocean circulation, *J. Clim.*, *15*, 470–486.

Nakamura, H., G. Lin, and T. Yamagata (1997), Decadal climate variability in the North Pacific in recent decades, *Bull. Am. Meteorol. Soc.*, *78*, 2215–2226.

Newman, M., and P. D. Sardeshmukh (1998), The impact of the annual cycle on the North Pacific/North American response to remote low frequency forcing, *J. Atmos. Sci.*, *55*, 1336–1353.

Newman, M., G. P. Compo, and M. A. Alexander (2003), ENSO-forced variability of the Pacific Decadal Oscillation, *J. Clim.*, *16*, 3853–3857.

Nigam, S. (2003), Hadley circulation, in *Encyclopedia of Atmospheric Sciences*, edited by J. R. Holton et al., pp. 2243–2268, Elsevier, New York.

Nitta, J. (1987), Convective activities in the tropical western Pacific and their impact on the Northern Hemisphere summer circulation, *J. Meteorol. Soc. Jpn.*, *65*, 373–390.

Nonaka, M., and S.-P. Xie (2000), Propagation of North Pacific interdecadal subsurface temperature anomalies in an ocean GCM, *Geophys. Res. Lett.*, *27*, 3747–3750.

Norris, J. R. (2000), Interannual and interdecadal variability in the storm track, cloudiness, and sea surface temperature over the summertime North Pacific, *J. Clim.*, *13*, 422–430.

Norris, J. R., and C. Leovy (1994), Interannual variability in stratiform cloudiness and sea surface temperature, *J. Clim.*, *7*, 1915–1925.

Oort, A. H., and J. J. Yieneger (1996), Observed interannual variability in the Hadley circulation and the connection to ENSO, *J. Clim.*, *9*, 2751–2767.

Paparella, F., and W. R. Young (2002), Horizontal convection is non turbulent, *J. Fluid Mech.*, *466*, 205–214.

Park, S., and C. B. Leovy (2004), Marine low-cloud anomalies associated with ENSO, *J. Clim.*, *17*, 3448–3469.

Pedlosky, J. (1984), Cross-gyre ventilation of the subtropical gyre: An internal mode in the ventilated thermocline, *J. Phys. Oceanogr.*, *14*, 1172–1178.

Pedlosky, J. (1987a), *Geophysical Fluid Dynamics*, 710 pp., Springer, New York.

Pedlosky, J. (1987b), An inertial theory of the equatorial undercurrent, *J. Phys. Oceanogr.*, *17*, 1978–1985.

Peixoto, J. P., and A. H. Oort (1992), *Physics of Climate*, Am. Inst. of Phys., College Park, Md.

Peng, S., and W. A. Robinson (2001), Relationships between atmospheric internal variability and the responses to an extratropical SST anomaly, *J. Clim.*, *14*, 2943–2959.

Peng, S., and J. S. Whitaker (1999), Mechanisms determining the atmospheric response to midlatitude SST anomalies, *J. Clim.*, *12*, 1393–1408.

Peng, S., W. A. Robinson, S. Li, and M. P. Hoerling (2005), Tropical Atlantic SST forcing of coupled North Atlantic seasonal responses, *J. Clim.*, *18*, 480–496.

Perlwitz, J., and N. Harnik (2004), Downward coupling between the stratosphere and troposphere: The relative roles of wave and zonal mean processes, *J. Clim.*, *24*, 4902–4909.

Philander, S. G. H., and R. C. Pacanowski (1980), The generation of equatorial currents, *J. Geophys. Res.*, *85*, 1123–1136.

Pierce, D. W., T. P. Barnett, and M. Latif (2000), Connections between the Pacific Ocean tropics and midlatitudes on decadal timescales, *J. Clim.*, *13*, 1173–1194.

Pierrehummbert, R. T. (1995), Thermostats, radiator fins, and the local runaway greenhouse, *J. Atmos. Sci.*, *52*, 1784–1806.

Quan, X.-W., H. F. Diaz, and M. P. Hoerling (2004), Changes in the tropical Hadley cell since 1950, in *The Hadley Circulation: Pre-*

sent, Past, and Future, *Adv. Global Change Res.*, vol. 21, edited by H. F. Diaz and R. S. Bradley, pp. 85–120, Springer, New York.

Rahmstorf, S. (1996), On the freshwater forcing and transport of the Atlantic thermohaline circulation, *Clim. Dyn.*, *12*, 799–811.

Randel, W. J., and I. M. Held (1991), Phase speed spectra of transient eddy fluxes and critical layer absorption, *J. Atmos. Sci.*, *48*, 688–697.

Raphael, M. N. (2004), A zonal wave 3 index for the Southern Hemisphere, *Geophys. Res. Lett.*, *31*, L23212, doi:10.1029/2004GL020365.

Rasmusson, E. M., and K. Mo (1993), Linkages between 200-mb tropical and extratropical circulation anomalies during the 1986–1989 ENSO cycle, *J. Clim.*, *6*, 595–616.

Rhines, P. B., and W. R. Young (1982), A theory of the wind-driven circulation. I. Mid-ocean gyres, *J. Mar. Res.*, *40*, suppl., 559–596.

Richman, M. B. (1986), Rotation of principal components, *J. Climatol.*, *6*, 293–335.

Robertson, A. W., and C. R. Mechoso (2003), Circulation regimes and low-frequency oscillations in the South Pacific sector, *Mon. Weather Rev.*, *131*, 2540–2551.

Robinson, W. A. (2000), A baroclinic mechanism for the eddy feedback on the zonal index, *J. Atmos. Sci.*, *57*, 415–422.

Rochford, P. A., A. B. Kara, A. J. Wallcraft, and R. A. Arnone (2001), Importance of solar subsurface heating in ocean general circulation models, *J. Geophys. Res.*, *106*, 30,923–30,938.

Rodgers, K., M. A. Cane, N. Naik, and D. Schrag (1999), The role of the Indonesian Throughflow in equatorial Pacific thermocline ventilation, *J. Geophys. Res.*, *104*, 20,551–20,570.

Rooth, C. (1982), Hydrology and ocean circulation, *Prog. Oceanogr.*, *11*, 131–149.

Ruddiman, W. F. (2001), *Earth's Climate: Past and Future*, 465 pp., W. H. Freeman, New York.

Rumford, B. (1800), Essay VII, the propagation of heat in fluids, in *Essays, Political, Economical, and Philosophical, A New Edition*, vol. 2, edited by T. Cadell Jr. and W. Davies, pp. 197–386, Manning and Loring, Boston, Mass.

Saji, N. H., and T. Yamagata (2003), Structure of SST and surface wind variability during Indian Ocean dipole mode events: COADS observations, *J. Clim.*, *16*, 2735–2751.

Saji, N. H., B. N. Goswami, P. N. Vinayachandran, and T. Yamagata (1999), A dipole mode in the tropical Indian Ocean, *Nature*, *401*, 360–363.

Sardeshmukh, P. D., and B. J. Hoskins (1985), Vorticity balances in the tropics during the 1982–83 El Niño–Southern Oscillation event, *Q. J. R. Meteorol. Soc.*, *111*, 261–278.

Sardeshmukh, P. D., and B. J. Hoskins (1988), The generation of global rotational flow by steady idealized tropical divergence, *J. Atmos. Sci.*, *45*, 1228–1251.

Sardeshmukh, P. D., G. P. Compo, and C. Penland (2000), Changes of probability associated with El Niño, *J. Clim.*, *13*, 4268–4286.

Sarmiento, J. L., and J. R. Toggweiler (1984), A new model for the role of the oceans in determining atmospheric pCO_2, *Nature*, *308*, 621–624.

Schmittner, A., O. A. Saenko, and A. J. Weaver (2003), Coupling of the hemispheres in observations and simulations of glacial climate change, *Quat. Sci. Rev.*, *22*, 659–671.

Schneider, E. K., and I. G. Watterson (1984), Stationary Rossby wave propagation through easterly layers, *J. Atmos. Sci.*, *41*, 2069–2083.

Schneider, N. (2000), A decadal spiciness mode in the tropics, *Geophys. Res. Lett.*, *27*, 257–260.

Schneider, N., and B. D. Cornuelle (2005), The forcing of the Pacific Decadal Oscillation, *J. Clim.*, *18*, 4355–4373.

Schneider, N., A. J. Miller, M. A. Alexander, and C. Deser (1999), Subduction of decadal North Pacific temperature anomalies: Observations and dynamics, *J. Phys. Oceanogr.*, *29*, 1056–1070.

Schopp, R. (1988), Spinup toward communication between large oceanic subpolar and subtropical gyres, *J. Phys. Oceanogr.*, *18*, 1241–1259.

Schott, F., M. Dengler, and R. Schoenefeldt (2002), The shallow thermohaline circulation of the Indian Ocean, *Prog. Oceanogr.*, *53*, 57–103.

Schott, F. A., J. P. McCreary, and G. C. Johnson (2004), Shallow overturning circulations of the tropical-subtropical oceans, in *Earth's Climate: The Ocean-Atmosphere Interaction*, *Geophys. Monogr. Ser.*, vol. 147, edited by C. Wang, S.-P. Xie, and J. A. Carton, pp. 261–304, AGU, Washington, D. C.

Scott, J., P. H. Stone, and J. Marotzke (1999), Interhemispheric thermohaline circulation in a coupled box model, *J. Phys. Oceanogr.*, *29*, 165–351.

Seager, R., and R. Murtugudde (1997), Ocean dynamics, thermocline adjustment and regulation of tropical SST, *Clim, J.*, *10*, 521–534.

Seager, R., N. Harnik, Y. Kushnir, W. Robinson, and J. Miller (2003), Mechanisms of hemispherically symmetric climate variability, *J. Clim.*, *16*, 2960–2978.

Shackleton, N. (2000), The 100,000-year ice-age cycle identified and found to lag temperature, carbon dioxide, and orbital eccentricity, *Science*, *289*, 1897–1902.

Shin, S., and Z. Liu (2000), Response of equatorial thermocline to extratropical buoyancy forcing, *J. Phys. Oceanogr.*, *30*, 2883–2905.

Shin, S., Z. Liu, B. Otto-Bliesner, E. Brady, J. Kutzbach, and S. Vavrus (2003), Southern Ocean sea-ice control of the glacial North Atlantic thermohaline circulation, *Geophys. Res. Lett.*, *30*(2), 1096, doi:10.1029/2002GL015513.

Shinoda, T., H. H. Hendon, and M. A. Alexander (2004), Surface and subsurface dipole variability in the Indian Ocean and its relation with ENSO, *Deep Sea Res., Part I*, *51*, 619–635.

Simmons, A. J., J. M. Wallace, and G. W. Branstator (1983), Barotropic wave propagation and instability, and atmospheric teleconnection patterns, *J. Atmos. Sci.*, *40*, 1363–1392.

Solomon, A., J. P. McCreary, R. Kleeman, and B. A. Klinger (2003), Interannual and decadal variability in an intermediate coupled model of the Pacific region, *J. Clim.*, *16*, 383–405.

Steig, E. J., and R. B. Alley (2003), Phase relationships between Antarctic and Greenland climate records, *Ann. Glaciol.*, *35*, 451–456.

Stephens, B. B., and R. F. Keeling (2002), The influence of Antarctic sea ice on glacial-interglacial CO_2 variations, *Nature*, *404*, 171–174.

Stephens, M., Z. Liu, and H. Yang (2001), On the evolution of subduction planetary waves with application to Pacific decadal thermocline variability, *J. Phys. Oceanogr.*, *31*, 1733–1746.

Stocker, T. F. (2000), Past and future reorganizations in the climate system, *Quat. Sci. Rev.*, *19*, 301–319.

Stommel, H. (1958), The abyssal circulation, *Deep Sea Res*, *5*, 80–82.

Stommel, H. (1960), *The Gulf Stream*, Univ. of Calif. Press, Berkeley.

Stommel, H. (1961), Thermohaline convection with two stable regimes of flow, *Tellus*, *13*, 224–241.

Stommel, H., and A. B. Arons (1960), On the abyssal circulation of the world ocean—I. Stationary planetary flow patterns on a sphere, *Deep Sea Res.*, *6*, 140–154.

Stommel, H., and K. Yoshida (1972), *Kuroshio: Its Physical Aspects*, Univ. of Tokyo Press, Tokyo.

Stouffer, R. (2004), Time scales of climate response, *J. Clim.*, *17*, 209–217.

Sutton, R. T., S. P. Jewson, and D. P. Rowell (2000), The elements of climate variability in the tropical Atlantic region, *J. Clim.*, *13*, 3261–3284.

Sverdrup, H. U. (1947), Wind-driven currents in a baroclinic ocean: With application to the equatorial currents of the eastern Pacific, *Proc. Natl. Acad. Sci. U. S. A.*, *33*, 318–326.

Thompson, D. W. J., and D. J. Lorenz (2004), The signature of the annular modes in the tropical troposphere, *J. Clim.*, *17*, 4330–4342.

Thompson, D. W. J., and J. M. Wallace (1998), The Arctic Oscillation signature in the wintertime geopotential height and temperature fields, *Geophys. Res. Lett.*, *25*, 1297–1300.

Thompson, D. W. J., and J. M. Wallace (2000), Annular modes in the extratropical circulation. part I: Month-to-month variability, *J. Clim.*, *13*, 1000–1016.

Ting, M., and I. Held (1990), The stationary wave response to a tropical SST anomaly in an idealized GCM, *J. Atmos. Sci.*, *47*, 2546–2566.

Ting, M., and P. D. Sardeshmukh (1993), Factors determining the extratropical response to equatorial diabatic heating anomalies, *J. Atmos. Sci.*, *50*, 907–918.

Ting, M., and H. Wang (1997), Summertime U.S. precipitation variability and its relation to Pacific sea surface temperature, *J. Clim.*, *10*, 1853–1873.

Toggweiler, J. R., and B. Samuels (1995), Effect of Drake Passage on the global thermohaline circulation, *Deep Sea Res., Part I*, *42*, 477–500.

Toggweiler, J. R., K. Dixon, and W. S. Broecker (1991), The Peru upwelling and the ventilation of the South Pacific thermocline, *J. Geophys. Res.*, *96*, 20,467–20,497.

Trenberth, K. E. (1990), Recent observed interdecadal climate changes in the Northern Hemisphere, *Bull. Am. Meteorol. Soc.*, *71*, 988–993.

Trenberth, K. E., and J. M. Caron (2001), Estimates of meridional atmosphere and ocean heat transports, *J. Clim.*, *14*, 3433–3443.

Trenberth, K. E., and A. Solomon (1994), The global heat balance: Heat transports in the atmosphere and ocean, *Clim. Dyn.*, *10*, 107–134.

Trenberth, K. E., G. W. Branstator, D. Karoly, A. Kumar, N.-C. Lau, and C. Ropelewski (1998), Progress during TOGA in understanding and modeling global teleconnections associated with tropical sea surface temperatures, *J. Geophys. Res.*, *103*, 14,291–14,324.

van Loon, H., and D. J. Shea (1987), The Southern Oscillation. part VI: Anomalies of sea level pressure on the Southern Hemisphere and of Pacific sea surface temperature during the development of a warm event, *Mon. Weather Rev.*, *115*, 370–379.

Vimont, D. J., D. S. Battisti, and A. C. Hirst (2001), Footprinting: A seasonal link between the mid-latitudes and tropics, *Geophys. Res. Lett.*, *28*, 3923–3926.

Vimont, D. J., J. M. Wallace, and D. S. Battisti (2003), The seasonal footprinting mechanism in the Pacific: Implications for ENSO, *J. Clim.*, *16*, 2668–2675.

Visser, K., R. Thunell, and L. Stout (2003), Magnitude and timing of Indo-Pacific warm pool during deglaciation, *Nature*, *421*, 152–155.

Vonder Haar, T. H., and A. H. Oort (1973), New estimate of annual poleward energy transport by Northern Hemisphere oceans, *J. Phys. Oceanogr.*, *3*, 169–172.

Waliser, D. E., and N. Graham (1993), Convective cloud systems and warm pool SSTs: Coupled interactions and self-regulation, *J. Geophys. Res.*, *98*, 12,881–12,893.

Waliser, D. E., Z. Shi, J. R. Lanzante, and A. H. Oort (1999), The Hadley circulation: Assessing NCEP/NCAR reanalysis and sparse in situ estimate, *Clim. Dyn.*, *15*, 719–735.

Walker, G. T. (1924), Correlation in seasonal variations of weather IX, *Mem. India Meteorol. Dep.*, *24*, 275–332.

Wallace, J. M., and D. S. Gutzler (1981), Teleconnections in the geopotential height field during the Northern Hemisphere winter, *Mon. Weather Rev.*, *109*, 784–812.

Wang, B., and X. Xie (1996), Low-frequency equatorial waves in vertically sheared zonal flow. part I: Stable waves, *J. Atmos. Sci.*, *53*, 449–467.

Wang, C. (2003), Atmospheric circulation cells associated with El Niño–Southern Oscillation, *J. Clim.*, *15*, 399–419.

Wang, D. X., and Z. Liu (2000), The pathway of interdecadal variability in the Pacific Ocean, *Chin. Sci. Bull.*, *45*, 1555–1561.

Wang, W., and R. X. Huang (2005), An experimental study on thermal circulation driven by horizontal differential heating, *J. Fluid Mech.*, *540*, 49–73.

Wang, X. L., P. H. Stone, and J. Marotzke (1999), Global thermohaline circulation. part I: Sensitivity to atmospheric moisture transport, *J. Clim.*, *29*, 71–82.

Wang, Y. J., H. Cheng, R. L. Edwards, Z. S. An, J. Y. Wu, C. C. Shen, and J. A. Dorale (2001), A high-resolution absolute-dated late Pleistocene monsoon record from Hulu Cave, China, *Science*, *294*, 2345–2348.

Warren, B. A. (1981), Deep circulation of the world ocean, in *Evolution of Physical Oceanography: Scientific Surveys in Honor of Henry Stommel*, edited by B. A. Warren and C. Wunsch, pp. 6–41, MIT Press, Cambridge, Mass.

Weaver, A. J., S. M. Aura, and P. G. Myers (1994), Interdecadal variability in an idealized model of the North Atlantic, *J. Geophys. Res.*, *99*, 12,423–12,441.

Weaver, A. J., O. A. Saenko, P. U. Clark, and J. X. Mitrovica (2002), Meltwater pulse 1A from Antarctica as a trigger of the Bølling-Allerød warm interval, *Science*, *299*, 1645–1709.

Webster, P. J., and J. R. Holton (1982), Cross-equatorial response to middle-latitude forcing in a zonally varying basic state, *J. Atmos. Sci.*, *39*, 722–733.

Wu, L., Z. Liu, and R. Gallimore (2001), Pacific interdecadal variability in a coupled model, in *Dynamics of Atmospheric and Oceanic Circulations and Climate*, edited by B. Wang, pp. 486–507, China Meteorol. Press, Beijing.

Wu, L., Z. Liu, R. Gallimore, R. Jacob, D. Lee, and Y. Zhong (2003), A coupled modeling study of Pacific decadal variability: The Tropical Mode and the North Pacific Mode, *J. Clim.*, *16*, 1101–1120.

Wu, L., D. Lee, and Z. Liu (2005), The 1976/77 North Pacific climate regime shift: The role of subtropical ocean adjustment and coupled ocean-atmosphere feedbacks, *J. Clim.*, *18*, 5125–5140.

Wu, L., Z. Liu, and C. Li (2007), Extratropical control of recent tropical Pacific decadal climate variability: A relay teleconnection, *Clim. Dyn.*, *28*, 99–112, doi:10.1007/s00382-006-0198-5.

Wunsch, C. (2003), Greenland-Antarctic phase relations and millennial time-scale climate fluctuations in the Greenland ice-cores, *Quat. Sci. Rev.*, *22*, 1631–1646.

Wunsch, C. (2005), The total meridional heat flux and its oceanic and atmospheric partition, *J. Clim.*, *18*, 4374–4380.

Wunsch, C., and R. Ferrari (2004), Vertical mixing, energy, and the general circulation of the oceans, *Annu. Rev. Fluid Mech.*, *36*, 281–314.

Xie, P., and P. A. Arkin (1997), Global precipitation: A 17-year monthly analysis based on gauge observations, satellite estimates, and numerical model outputs, *Bull. Am. Meteorol. Soc.*, *78*, 2539–2558.

Xie, S.-P., and Y. Tanimoto (1998), A pan-Atlantic decadal climate oscillation, *Geophys. Res. Lett.*, *25*, 2185–2188.

Xie, S.-P., H. Annamalai, F. A. Schott, and J. P. McCreary (2002), Structure and mechanisms of south Indian Ocean climate variability, *J. Clim.*, *15*, 864–878.

Yang, H., and Z. Liu (1997), Three-dimensional chaotic ocean transport: The great ocean barrier, *J. Phys. Oceanogr.*, *27*, 1258–1273.

Yang, H., and Z. Liu (2005), Tropical-extratropical climate interaction as revealed in idealized coupled climate model experiments, *Clim. Dyn.*, *24*, 863–879.

Yang, H., Q. Zhang, Y. Zhong, S. Vavrus, and Z. Liu (2005), How does extratropical warming affect ENSO?, *Geophys. Res. Lett.*, *32*, L01702, doi:10.1029/2004GL021624.

Yang, J. (1999), A linkage between decadal climate variations in the Labrador Sea and the tropical Atlantic Ocean, *Geophys. Res. Lett.*, *26*, 1023–1026.

Yin, J., and D. Battisti (2001), The importance of tropical sea surface temperature patterns in simulations of Last Glacial Maximum climate, *J. Clim.*, *14*, 565–581.

Yuan, D., et al. (2004), Timing, duration, and transitions of the last interglacial Asian monsoon, *Science*, *304*, 575–578.

Zhang, D., M. J. McPhaden, and W. E. Johns (2003), Observational evidence for flow between the subtropical and tropical Atlantic: The Atlantic tropical cells, *J. Phys. Oceanogr.*, *33*, 1783–1797.

Zhang, R., and T. Delworth (2005), Simulated tropical response to a substantial weakening of the Atlantic thermohaline circulation, *J. Clim.*, *18*, 1853–1860.

Zhang, Y., J. M. Wallace, and D. S. Battisti (1997), ENSO-like interdecadal variability: 1900–1993, *J. Clim.*, *10*, 1004–1020.

M. Alexander, Physical Science Division, Earth System Research Laboratory, NOAA, 325 Broadway, Boulder, CO 80305-3328, USA.

Z. Liu, Center for Climatic Research, University of Wisconsin-Madison, 1225 W. Dayton Street, Madison, WI 53706-1695, USA. (zliu3facstaff. wisc.edu)